Analysis Of Energy Flow In Controlled Structures Subject To Initial Conditions

by

Darrell Scott McAlister

Thesis submitted to the Faculty of the

Virginia Polytechnic Institute and State University

in partial fulfillment of the requirements for the degree of

MASTER OF SCIENCE

in

Mechanical Engineering

APPROVED:

H. H. Robertshaw, Chairman

R. G. Leonard

W. R. Saunders

February, 1995
Blacksburg, Virginia

ANALYSIS OF ENERGY FLOW IN CONTROLLED STRUCTURES SUBJECT TO INITIAL CONDITIONS

by

Darrell S. McAlister

Committee Chairman: Harry H. Robertshaw

Mechanical Engineering

(ABSTRACT)

This work investigates power flow and energy transfer in controlled structures. If the goal of control is to stop an initially vibrating structure, energy must be forced out through dissipating components. The analysis performed here quantifies energy being transferred internally and externally to dissipative mechanisms in the primitives of a spring-mass-damper system and a beam-piezoelectrics-electronics system over the transient period of the systems' response to initial conditions.

The systems studied were broken down into capacitive, inertial, resistive and sourcing primitives. All systems containing primitives from all domains can be modeled this way. The analysis started from first principles and investigated energy flow in general. Energy flowing from the mechanical primitives to the electrical primitives is especially important because controlled structures often integrate primitives from these two domains.

Computer simulations showed that power seemingly flows into sources used to control the structures. This work also laid the groundwork for the development of control design methods based on energy flow.

Acknowledgments

First of all, I would like to thank Dr. Robertshaw for getting me through this program. Without your help I would have given up after my second semester. You were more than an academic advisor, you are a friend as well. I would also like to thank Dr. Saunders and Dr. Leonard for serving on my committee.

Thanks goes to everyone in the lab - to Dan Cole for his technical expertise, to Ben for his unique views on life, to Tom "the proof-reader" Snyder, to Pete Tappert and to Dan Miller. We have shared a lot, and I will never forget any of you.

I would like to thank my parents for always encouraging me and being there and for their financial support during my seven and a half years of school.

Most of all, I would like to thank my wife, Amy, for her unconditional support. For better and for worse, you are always there. You put up with a lot these last two years, and I will always love you for it.

Contents

List of Symbols

Symbol	Definition	Units
A,B,C,D	system state space equation (SSE) matrices	
a	piezoelectric endpoint along x coordinate	meters - m
c	damping coefficient	N/m/s
C_f	feedback capacitance	Farads - F
C_p	capacitance matrix	F
$\mathfrak{D}$, Damp	damping coefficient matrix	N/m/s
E	elastic modulus	N/m
	energy	Joule - J
e	effort variable	
f	flow variable	
	force	Newtons - N
h	width	m
I	area moment of inertia	m^4
I_q	op-amp quiscent supply current	amps
i	electrical current	amps
K	structural stiffness matrix	N/m
k	operational amplifier (op-amp) open loop gain	
l	beam length	m
M	mass matrix	kilograms - kg
m	mass per unit length	kg/m
n	number of points specifying a function	
N	transformer or gyrator constant	
	number of retained modes	
P	power	J/s
q	electrical charge	Coulomb - C
R	electrical resistance	Ohms - Ω
r	generalized displacement coordinate	
S	first area moment	m^3
T	kinetic energy	J
t	thickness	m
	time seconds	s
U	dissipated energy	J
V	potential energy	J
V_{cc}	op-amp rail voltage	V
v	voltage	Volts - V
	velocity	m/s
X	vector of state variables	

List of Symbols

Symbol	Definition	Units
x,y,z	cartesian coordinates	
Z	impedence	Ω
δ	Dirac delta function	
f	frequency	Hertz - Hz
λ	natural frequency	rad/s
Θ	electro-mechanical coupling matrix	N/V
Ψ	shape function matrix	
ω	frequency	rad/s
ζ	damping factor or ratio	

subscripts:

i	input
o	output
n	mode number
p	piezoelectric
s	structure (beam)

superscripts:

T	matrix transpose

List of Figures

List of Tables

Chapter 1

Introduction

The object of a structural control problem is often to reduce motion caused by external conditions. When a structure has some initial displacement or velocity, there exists some initial energy. If the control goal is to reduce the motion of the structure completely, the structure will have no final energy. In order to best meet the design criteria it seems important to know how the energy left the structure. It may be the goal of the designer to force the energy out of the system in a specified time or through a certain "port." A port is a location where energy may pass into or out of a system. Energy can only be identified at ports, and the quantity of energy which has passed into or out of a port is the time integral of the power flowing through the port due to system variables:

$$E = \int P dt .$$

In other words, power is the time rate of energy. Therefore, we speak of power as a flow rate at a particular time and energy as a quantity transferred into or out of a component over a particular length of time. Initial energy is a quantity referred to in this work to specify energy initially stored in the system that would leave over the transient period.

Energy can be calculated from system variables through the expression for power: $P(t) = e(t) \cdot f(t)$. The system variables e(t) and f(t), also known as the system's power duals, are present in any type of system, or domain, in which power flows, including mechanical, electrical, hydraulic and magnetic. The effort variable characterizes the potential for energy transfer, while the flow variable characterizes the rate of energy transfer. As an example, consider the mechanical translation variable force and its power dual velocity. Force is the effort variable and velocity is the flow variable. The commonly held expression for kinetic energy for a translating mechanical system is $T = \frac{1}{2} mv^2$. This follows from the fact that the expression for power in this system is $P = f \cdot v$, where all variables depend on time. Newton's law tells us that

$$f = m \cdot a = m \frac{dv}{dt} .$$

Consequently,

$$P = m \cdot v \frac{dv}{dt} ,$$

and

$$E = \int P dt = \int mv dv = m \int v dv = \tfrac{1}{2} mv^2 ,$$

where this expression is evaluated from some initial velocity v_1 to some final velocity v_2.

The goal of this work is to investigate energy transfer and power flow in controlled, dynamic systems and make recommendations on control design methods based on energy transfer and power flow methods. To achieve the goal, the flow of energy in some simple systems was simulated. Various control laws were added to the systems, and the

changing energy patterns were noted. As control law parameters are changed in a controlled system, the system responds to inputs and/or disturbances differently. The energy transfer changes course accordingly, and by adjusting these parameters, energy can be forced out of the system in a number of configurations. The transfer of energy in a cantilevered beam controlled by a pair of piezoelectric ceramics, or piezoelectrics, was also simulated. This system was chosen because it contains electrical and mechanical components, and the piezoelectrics convert mechanical energy to electrical energy and vice versa. This system also contains electrical components that appear in most control applications.

To get a thorough understanding of the energy transfer in a dynamic system, the system must first be broken down into subsystems and then into components or primitives. The primitives that make up a realistic system usually cross many domains; that is, they contain mechanical components, electrical components, hydraulic components, etc. The advantage of this modeling method is that it is general. The primitives described below exist in all domains.

The first primitive to be defined is the resistor. All primitives have corresponding laws called constitutive equations that relate effort and flow at the primitives' ports. The constitutive equation for a resistive primitive involves a static relationship between effort and flow. For example, the constitutive equation for the electrical resistor is $v = i \cdot R$, where v is the voltage (effort) across the resistor, and i is the current (flow) through the resistor. If the proportionality constant is positive, which it usually is, then energy is dissipated through this primitive. While the resistive primitive is nonconserving, the second

and third set of primitives, capacitors and inertias, store and give up energy without loss and are therefore referred to as conservative.

Energy related to capacitive primitives is known as potential energy, while energy related to inertial primitives is known as kinetic energy. In the mechanical domain, potential energy and kinetic energy are commonly thought of as energy of position and energy of motion, because they deal with displacement and velocity, respectively. When only conservative primitives are present, the sum of the energies into and out of these primitives over any time period is constant. This is commonly referred to as conservation of energy, and is used to solve simple dynamics problems involving springs, masses, pendulums, etc. When nonconservative primitives are involved, the sum of kinetic and potential energies does not remain constant because energy is flowing into and out of nonconservative primitives. But, of course, energy is always conserved if energy transfer among all primitives present in the system is considered. Both Bernoulli and Lagrange noted the conservation of mechanical energy over two centuries ago, and soon after, Joule and von Mayer discovered that all forms of energy are conserved (Hoffman, 1977).

The constitutive equation for a capacitive primitive involves a static relationship between effort and displacement, the time integral of flow. For example, a capacitive primitive in the mechanical domain is a spring, and its constitutive equation relates force to linear displacement, the time integral of velocity. The constitutive equation for an inertia involves a static relationship between effort and acceleration, the time derivative of flow. For example, a mechanical inertial primitive is a mass, and its constitutive equation relates

force to acceleration, the time derivative of velocity. Keep in mind that although displacement and acceleration are usually known as mechanical variables, analogous variables exist in all domains. The sign convention for the three basic 1-port primitives described above is: power is positive when it flows into a component and negative when it flows out. Initial energy is calculated from initial conditions affecting these two types of primitives. The expression calculated earlier for inertial primitives, $KE = \frac{1}{2}mf^2$ where f is the flow variable and m is an inertial constant, evaluated at the initial flow value plus the expression for capacitive primitives, $PE = \frac{1}{2}kx^2$ where x is the displacement or integral of flow and k is a capacitive constant, is the total initial conservative energy in the system. This energy is lost through dissipative primitives (resistors and sources) as the system settles to a no-energy state.

Multiport primitives allow power to flow in and out through more than one port. There are only a few unique multiports that cannot be defined using the 1-port primitives discussed above. All multiports used in this work are assumed to be power conserving; that is, power flowing in equals power flowing out. Two common, unique 2-port components are the transformer and the gyrator. The constitutive law for the transformer is $e_1 = N \cdot e_2$, and since this component is power conserving, $N \cdot f_1 = f_2$. The gyrator's constitutive law is $e_1 = N \cdot f_2$, and since this component is power conserving, $N \cdot f_1 = e_2$. N is a constant. Using the 1-port and multiport components described above and connector laws like Kirchoff's current law (KCL), systems can be modeled in a way that allows for simple energy analysis.

Effort and flow sources make up another set of primitives, and since these primitives are usually thought of as supplying power to the system, the sign convention is: power is positive when it flows from the source. Note that this is opposite to the sign convention for the three non-source primitive sets described above. An example of an effort source from the electrical domain is a battery. While the voltage of an ideal battery remains constant, the current varies depending on the load. The defining feature of these source primitives is that effort and flow are independent over the entire power range; of course, this is unrealistic. Ideal models of real sources are also often unrealistic because the load can command any power flow without limit. If not accounted for, ideal resistive primitives can also dissipate any amount of power. This is untrue, and power levels must be known to properly design a control system.

After considering the 1-port and source primitives, it is apparent that there are three kinds of power flowing in systems: dissipated, reactive and supplied. Dissipative power is power that leaves the system through a primitive as heat, sound, etc, while reactive power is power that is transformed, back and forth, between domains, e.g., mechanical and electrical. Supplied power is a more mysterious form of power because the source is often not obviously connected to the system. A wall outlet is an example of an electrical source. In addition, the concept of power flowing into a source is ambiguous. Does the source dissipate energy? As shown later, the source must "absorb" energy in order for the system to obey the law of energy conservation. This is an important issue in this thesis, and it is discussed in detail later.

One of the objectives of this work is to model sources, actuators, sensors and

other control components using the primitives described above. Another objective of this work is to discover how energy moving from one component to another affects the other components in the system. The conversion of mechanical energy to electrical energy is an important issue because control systems often integrate the two domains. Piezoelectric elements are important because they transfer power from mechanical systems to electrical components, and since all electronic components have maximum power ratings, it is important to correctly model power flow through these elements.

Chapter 2

Literature Review

Recent research has noted that an understanding of the power flow in structures integrated with piezoelectrics, piezostructures, is important because piezoelectric actuators and sensors place often unknown requirements on the electronic components which drive them (Warkentin and Crawley, 1994). It is obviously true that electronic components all have maximum power ratings, and if the purpose of feedback control is to damp a vibrating system, electronic components will have to dissipate a certain amount of energy or sink a certain amount of power. With the increasing use of piezoelectric components to control flexible structures, a better understanding of power flow through these components is required in order to meet the maximum power ratings of connected electronic components. This author also notes that power flow in piezoelectric components is important because it has been largely neglected until recently.

The other recent work investigating energy transfer and power flow in piezoelectric actuators was conducted by the Liang, Sun and Rogers (1993 and 1994). In these works an effort was made to quantify both mechanical and electrical power flow for piezoelectrically actuated structures. An electro-mechanical impedance method was used in

these papers that requires knowledge of impedance corresponding to actuator load. Since impedance relates effort and flow, power can be calculated if either the effort or the flow variable is known. Warkentin and Crawley (1994) point out that the derivation of various impedances is not always straightforward. They present a method that can be extended to complex systems using energy or finite element methods, for example. Unlike the Liang, Sun and Rogers work, the Warkentin and Crawley paper does not contain expressions for mechanical energy flowing between the actuator and structure. It focuses on energy flowing between control components like amplifiers and piezoelectric actuators.

Liang, Sun and Rogers (1993, 1994) note that it is also important to find expressions for power consumption in order to optimize an intelligent material system based on minimizing a power consumption function. Therefore, optimization is also a major motivating factor in the search for realistic power flow and energy transfer expressions in controlled structures. To suppress movement in structures it is logical to try to minimize the energy in the system. Controller optimization techniques have used energy performance measures like minimizing the system energy (Kirby, Matic and Lindner 1994; Yang and Lee, 1993 and Schulz and Heimbold, 1983) and maximizing the energy dissipated in the system (Miller and Shim, 1987). Although energy optimization does not directly relate to what has been studied here, it involves energy transfer expressions and is therefore discussed briefly when dealing with the simple systems.

Most of the current work involves energy transfer and power flow in piezoelectrically actuated smart structures, while a more general approach is taken in this work. The

approach taken in the papers discussed above is altogether different. Here, the problem was approached from first principles. Looking at general power flow in controlled structures helped give insight into how power flows into and out of power sources. The general modeling method used here was taken from Karnopp and Rosenberg (1975), who used a modeling approach they believe is the most unified and understandable way to get analytical and computational results from complex systems involving a variety of types of energy transfer. They develop the concept that systems contain components that receive energy from and give energy to connected components through ports. Energy transfer and power flow methods offer a unique way of looking at control systems and offer unexplored options in the field of controls.

Chapter 3

Modeling

A general method was used to model the energy transfer in the systems discussed here. The method consists of breaking the system down into components and then into the primitives discussed in the introduction and then looking at the power variables at the ports of these primitives. Before power flow and energy transfer can be modeled and quantified, the system dynamics must be modeled. First, dynamics and energy transfer were modeled in some simple spring-mass-damper (SMD) systems. Then the beam-piezoelectrics-electronics (BPE) system was modeled because it contains components commonly used in control applications.

3.1 Simple Systems

Power flow and energy transfer were investigated in SMD systems with varying primitive constants as a first step towards gaining a better understanding of energy transfer in more complicated, realistic systems. Energy transfer in these simple systems is easy to visualize and easy to simulate since there are only a few energy dissipation and storage

devices present, and they are all members of the mechanical domain. A damper is a resistive device, and therefore, its constitutive equation relates the effort variable to the flow variable by a multiplication constant, the viscous friction coefficient. Since the viscous friction coefficient is always positive, the signs of the power variables are always the same, and consequently, the damper always dissipates or removes energy from the system. As noted in the introduction, a spring is a capacitive device because its constitutive equation relates the effort variable to displacement by a multiplication constant, the spring constant. Since the power calculation of this device depends on the integral of the flow variable, power may flow into or out of this device with no loss to the atmosphere. The third device present in these simple systems is an inertia. It takes the form of a mass, and the constitutive equation relates the effort variable to acceleration by a multiplication constant, the mass. An inertia is also a nondissipating energy storing device. The final device present in these systems is an effort source.

The primitive used to control the system is a source that comes in the form of a force acting on the mass. The effort source is ideal in the sense that it can produce any force required by the controller on demand, and that the mechanism in which energy is stored or dissipated in the source is not modeled. The control method employed in all cases is full state feedback. Linear Quadratic Regulator (LQR) design and pole placement were used to design the full state feedback control law. The root selection method was varied to observe the effect of pole location on energy transfer.

LQR is an optimal control method in which the following cost function:

$$J = \int_0^\infty (x^T Q x + u^T R u)\, dt$$

is minimized subject to the system (constraint) equation: $-\dot{x} + Ax + Bu = 0$. Solving this optimization problem results in another way of calculating the gain matrix, K, in the feedback control law $u = -Kx$. The square matrices Q and R are used to weight either the states x or the control u. The size of Q is equal to the order of the system or the number of state variables, and the size of R depends on the number of inputs to the system. Note in these simple systems R is a scalar since there is only one input.

As discussed in the literature review section of this thesis, there are optimal control methods based on energy transfer in the system. One group of optimal control methods involves the LQR cost function. The state vector x and the state weighting matrix Q can be altered so that $x^T Q x$ expresses the sum of the kinetic and potential energies of the system. If x is the vector of modal displacements and modal velocities, $x = [r_1, r_2, \ldots, r_N, \dot{r}_1, \dot{r}_2, \ldots, \dot{r}_N]^T$, and

$$Q = \tfrac{1}{2}\begin{bmatrix} K & 0_N \\ 0_N & M \end{bmatrix},$$

where 0_N is the N×N zero matrix, and N is the number of retained modes, the conservative energy in the system will be minimized due to nonconservative energy exiting the system through resistive primitives and sources. This only works if the states are defined properly. If there are other conservative primitives in the system, their associated energy transfer characteristics must be accounted for in the state weighting matrix. The system

could very easily become too complex to represent in the LQR form used above. Therefore, a better understanding of energy flow is necessary.

Before looking at energy transfer and power flow in a specific system, the power variables existing at every port in the system must be solved for. In these SMD systems, these variables are force and velocity. The state-space derivations for the simple systems investigated here are shown in Appendix A, and these derivations are a result of the application of Lagrange's equation. The control algorithms and time simulations for these systems have been encoded into MATLAB's programming language as script files (or m-files). The first m-file in Appendix C, `ENERGY1A.M`, calculates the system response due to initial conditions for simple SMD systems with various primitive configurations.

3.2 Beam-Piezoelectrics-Electronics (BPE) System

3.2.1 BPE Dynamics Modeling

The electro-mechanical interaction of a cantilevered beam with two surface-mounted piezoelectric pairs was modeled using the method developed by Hagood et al. (1990). This method results in coupled equations of motion for the structure with piezoelectric elements, the piezostructure. Figure 3.1 shows the BPE system, and Fig. 3.2 shows the dimensions of the piezostructure. Using this modeling method, power variables are easily solved for, and energy moving from the structure to the electronics through the

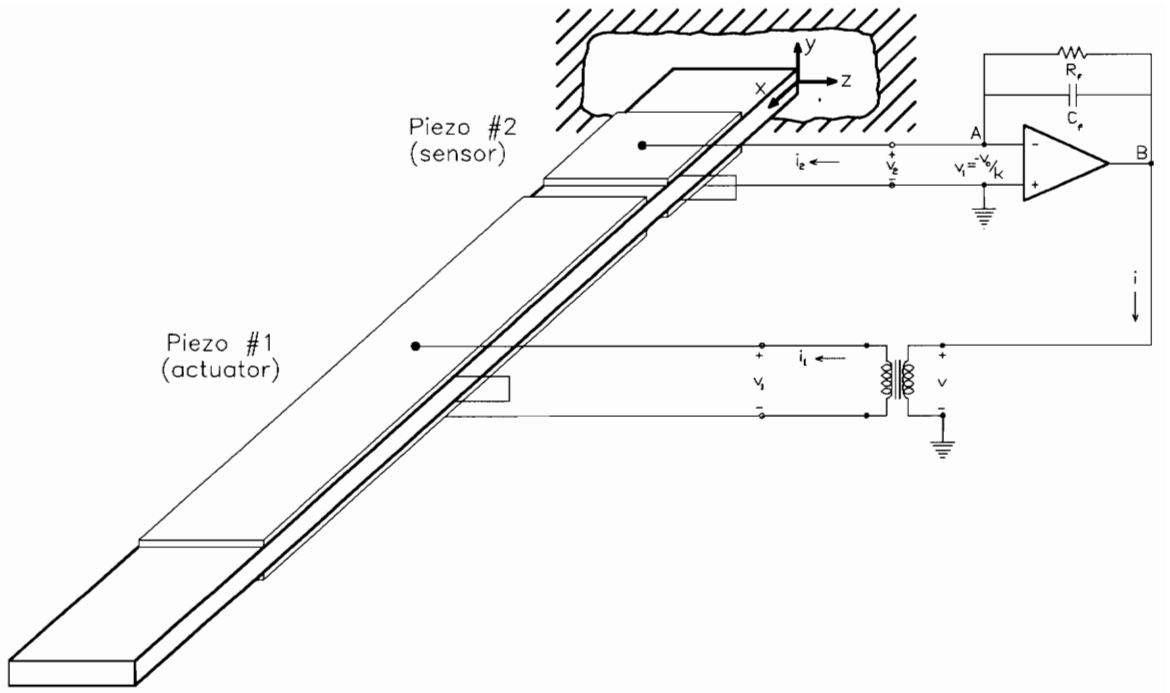

Figure 3.1: Beam-Piezoelectrics-Electronics (BPE) System

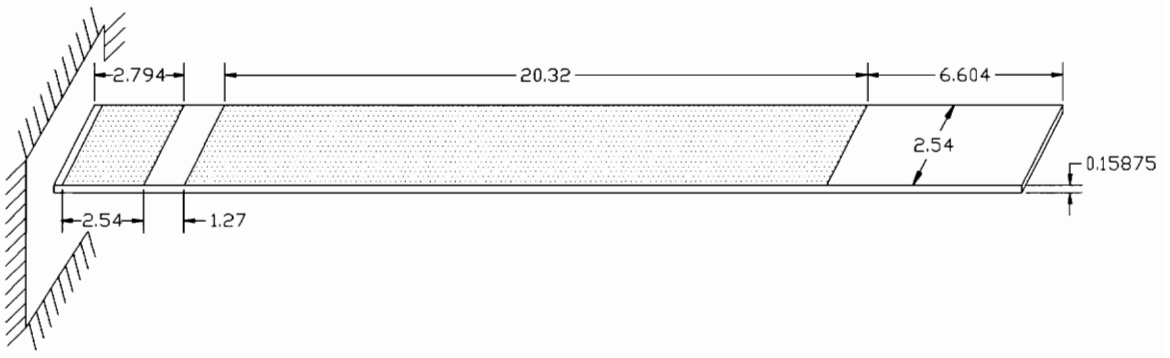

Figure 3.2: Piezostructure Dimensions (in centimeters)

piezoelectrics can be quantified and investigated. The material properties for the aluminum beam and G-1195 piezoelectric ceramics (Piezotronics Division of AIM Technologies, Inc.) are shown in Table 3.1.

Table 3.1: Material Properties of the Piezostructure

Beam Properties		
Elastic Modulus	E_s	$7.102 \cdot 10^{10}$ m.
Poisson's Ratio	ν_s	0.334
Mass Density	w_s	2768 kg/m^3
Damping Ratio (all modes)	ζ	0.01
Piezoelectric Properties		
Thickness	t_{p2}	$2.54 \cdot 10^{-4}$ m.
	t_{p1}	$5.08 \cdot 10^{-4}$ m.
Mass Density	w_p	$7.6 \cdot 10^3$ kg/m^3
Poisson's Ratio	ν_p	0.4
Elastic Modulus (x and z)	E_{px}	$5.292 \cdot 10^{10}$ Pa.
Elastic Modulus (y)	E_{py}	$4.8 \cdot 10^{10}$ Pa.
Strain Constants	d_{31}	$180 \cdot 10^{-12}$ m/V
	d_{33}	$360 \cdot 10^{-12}$ m/V

The piezoelectric pairs are mounted so that they work together to exert a bending moment on the beam if a voltage is applied across the two outside electrodes of the pair. The piezoelectric poling direction is along the y-axis as noted in Fig. 3.1. The poling direction shows the sense in which a moment will be applied from the piezoelectric if a voltage is placed across the electrodes. The inside of each piezoelectric is insulated from the beam and coupled electrically. Therefore, if both piezoelectrics share the same impedance to current, the voltage across each piezoelectric is half the voltage applied across the outside electrodes of the pair. The piezoelectric pair closest to the fixed end of the beam, pair

#1, is the actuator used to control the beam's response to initial conditions. The pair closest to the free end of the beam, pair #2, is the sensor. The voltage across pair #2 is fed back to pair #1 through the operational amplifier (op-amp) circuit and an appropriate gain. Before proceeding with piezostructure modeling, some important electronic circuit principles will be discussed.

This op-amp circuit is known as a charge amplifier because it takes the low output signal from the piezoelectric sensor and steps it up so it can be used to measure the beam's response to initial conditions. The charge amplifier views the sensor as a charge source and converts charge variations to voltage variations. Op-amps are also often used in control applications to drive actuators. The Warkentin and Crawley paper examines power consumption in an amplifier circuit used to drive a piezoelectric actuator. The overall amplifier configuration may differ from the charge amp configuration discussed here, but the op-amp is always present. The op-amp used here is set up like a charge amp, but is ultimately inserted into the feedback path to investigate power flow and energy transfer.

The ability of the charge amp to amplify charge depends on many factors. If the feedback resistor is ignored temporarily, the charge balance equation at node A (see Fig. 3.1) is

$$q_2 = -C_f\left(\frac{v_o}{k} + v_o\right)$$

An ideal op-amp has an open-loop gain of $k = \infty$. This reduces the above equation to

$$v_o = \frac{-q_2}{C_f}$$

If C_f is chosen appropriately, the charge at the op-amp input can be amplified greatly. The feedback resistor is necessary in a practical charge amp because, if it did not exist, input current flowing through the feedback capacitor would charge it up until the output saturates. The circuit will still act like a charge amp as long as the feedback resistance is high or the input frequency is high enough to make the impedance of the resistor much larger than the impedance of the capacitor. Frequency is a factor because the capacitor impedance is inversely proportional to frequency; $Z_c = 1/(j\omega C_f)$. Other practical considerations for implementing a charge amp in a controls application are discussed below.

When choosing appropriate feedback parameters for a charge amplifier, a few things must be kept in mind. First, the amplifier must have a time constant large enough to slow the charge leakage rate. Charge from the signal can leak out of the charge amp into the attached load before the amplifier does its job. The time constant for the charge amp used here is $\tau = R_f C_f$. Also, the time constant should be large in order to decrease the lower limit on frequency of operation. To achieve accuracy better than 99% for a properly calibrated charge amp, the minimum frequency of a transient signal should be $\omega_{min} = \frac{7.0}{\tau}$ (deSilva, 1989). Remember that a properly calibrated charge amp is one that obeys $v_o = \frac{-q_2}{C_f}$.

In addition to amplification, this op-amp circuit is often used to condition signals from piezoelectric transducers (deSilva, 1989). Signal conditioning circuits convert impedances between connected devices. If the output impedance of the first device is much

smaller than the input impedance of the second device, the devices are properly connected. If devices are not properly connected, signals can become distorted when passed from one component to another. In turn, inadequate and inaccurate output signals cause the controller to function improperly.

The term loading refers to the effect of improper connection of devices. If impedances are not appropriate, the errors become unacceptable. Figure 3.3 illustrates the connection of a two-port component with input and output impedances and a one port resistive load. The two-port component has an associated gain (constant or varying with

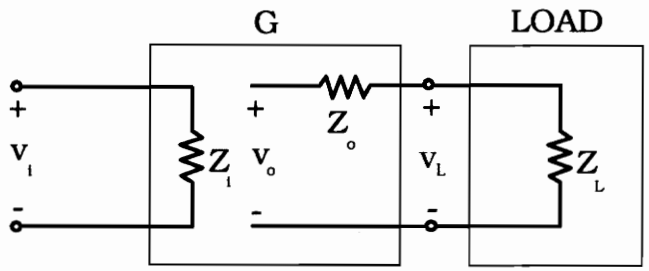

Figure 3.3: Connection of components to show loading effect

time), and the desired effect is to transform the input voltage v_i into the load voltage v_L by multiplying by the gain (transfer) function, $v_L = Gv_i$, but the impedances complicate things, and it is only true that $v_o = Gv_i$. Unless the designer has compensated for these impedances, the circuit will not function as designed. Elementary circuit analysis results in

$$v_L = G\frac{Z_L}{Z_o + Z_L}v_i$$

The ideal result, $v_L = Gv_i$, is reduced by the impedance ratio, but if $Z_o << Z_L$, the ideal result is approximately achieved. Op-amps posses this characteristic; that is, the input impedance is very high and the output impedance is very low, but the proper connection of components also depends on the impedances of the other devices in the chain. Care must be taken to ensure that the output impedance of the first device is much smaller than the input impedance of the second device in the chain. Since output impedances of piezoelectric sensors is very high, the input impedance of any component connected to it must be extremely high. Instead of the standard bipolar-junction transistor (BJT) op-amp, a field-effect transistor (FET) op-amp can be used to obtain higher input impedances, on the order of $10^{11}\ \Omega$ (Franco, 1988).

Piezoelectric sensors and actuators and electronic components such as the op-amp used here are often integrated and used in control because of the reasons described above. The specific application may require energy to flow in a certain manner, and the components must be able to dissipate the required energy. Therefore, it is important to know how energy moves from a piezoelectric to a charge amp and vice versa.

While modeling the interaction between the structure and piezoelectrics is straightforward (Hagood, Chung and von Flotow, 1990), modeling the interaction between the op-amp and the piezoelectrics is not. Because the typical op-amp uses many transistors, resistors and capacitors, a simplified model is necessary. For example, the popular Fairchild 741 op-amp is comprised of 20 BJTs, 11 resistors and 1 capacitor. Warkentin and Crawley use a transistor model to derive an expression for power dissi-

pated in a linear amplifier. But this model does not explain dissipation of power flowing into the amplifier rails. Since power was found to flow into the sources in the simple systems, power may flow into the op-amp rails in this system. But, how can power flow into the rails if they are constant voltage supplies? The Warkentin-Crawley model also does not account for the quiescent supply current, which is the current required to keep the internal transistors properly biased. The value of this current is constant for a particular op-amp and dependent on the op-amp type, supply voltage, etc. This power dissipation was found to be significant in some cases (Franco, 1988), but if the application requires the op-amp to sink a large amount of current, as in the case of a driving amplifier, the power dissipated by the quiescent supply current will be negligible. The first model chosen here is shown in Fig. 3.4. This is typically used in electronics textbooks (Franco, 1988; Bobrow, 1985 and deSilva, 1989). The rail or supply voltage which is used to power the amp has been omitted from this schematic since it is incorporated into the internal variable voltage source v_o. The problem with this model is that it does not incorporate the fact that the rail

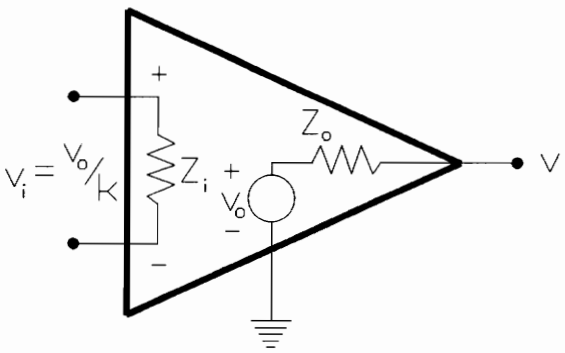

Figure 3.4: Variable Source Op-Amp Model

voltage is constant. The Warkentin-Crawley model has a constant supply voltage source, but also has the faults described above. Another model similar to the Warkentin-Crawley model is used for comparisons and is discussed later.

The assumptions usually made to obtain an ideal op-amp from the model in Fig. 3.4 are: $Z_i = \infty$ (open-circuit), $Z_o = 0$ ohms (short-circuit) and $k = \infty$. The current direction and voltage sign determine the direction of power flow. Power may flow into or out of the op-amp's output terminals. The resistive elements, Z_i and Z_o, assume values other than ∞ and 0 in a real op-amp. For the 741 op-amp used in these simulations, the values are: $Z_i = 2\ M\Omega$ and $Z_o = 75\ \Omega$. Since the constitutive equation for these primitives is $v = iZ$, where Z is a positive constant, the effort and flow variables, voltage and current, have the same sign. For resistive primitives, power is dissipated if the product of effort and flow is positive.

The mechanical part of this system, the piezostructure, is a distributed parameter system. The beam with integrated piezoelectrics is a distributed system because the mass, stiffness and damping are distributed throughout the structure's volume. Therefore, deflection in distributed parameter systems is a function of at least two variables, time and at least one direction. Consequently, these systems are defined by an infinite number of partial differential equations. The best way to deal with these systems, especially for computational design and control purposes, is to convert them into finite, lumped parameter systems, i.e., approximate the partial differential equations by a finite number of ordinary differential equations. This piezostructure is modeled like an eighth order (four degree-of-

freedom) lumped system; this results in a second order matrix equation. Using the Rayleigh-Ritz energy method, the matrix equations of motion for the piezostructure are

$$\text{actuator equation:} \qquad M\ddot{r} + C\dot{r} + Kr = \Theta v$$

$$\text{sensor equation} \qquad \Theta^T r + C_p v = q$$

where

$$M = \int_0^L \rho_s A_s \Psi_r^T \Psi_r \, \partial x + \int_{a_{i1}}^{a_{i2}} \rho_p A_p \Psi_r^T \Psi_r \, \partial x$$

$$K = \int_0^L (\Psi_r'')^T c_s I_s \Psi_r'' \, \partial x + \int_{a_{i1}}^{a_{i2}} (\Psi_r'')^T c_p I_p \Psi_r'' \, \partial x$$

$$\Theta = \sum_i \int_{a_{i1}}^{a_{i2}} (\Psi_r'')^T e_p S_p \begin{bmatrix} \delta_{1i} \dfrac{1}{t_p} & \delta_{2i} \dfrac{1}{t_p} \end{bmatrix} \partial x$$

$$C_p = \sum_i \int_{a_{i1}}^{a_{i2}} \begin{bmatrix} \delta_{1i} \dfrac{1}{t_p} \\ \delta_{2i} \dfrac{1}{t_p} \end{bmatrix} e_p A_p \begin{bmatrix} \delta_{1i} \dfrac{1}{t_p} & \delta_{2i} \dfrac{1}{t_p} \end{bmatrix} \partial x$$

where i is the piezoelectric index. The delta function, δ_{ji}, assumes the value one when the differentiation variable is over the i^{th} piezoelectric's length (i.e. when i=j) and zero otherwise (i.e. when $i \neq j$). Note that the integrals for the beam mass and stiffness matrices are over the beam length, and the integrals for the piezoelectric mass, stiffness, coupling and capacitance matrices are over the piezoelectric's length. The piezoelectric matrices are formed by summing the contribution from each piezoelectric element in the system (two

for this case). Note also that mass and stiffness matrices are calculated for the structure and the piezoelectrics separately. When summed, these matrices form the overall system mass and stiffness matrices. The capacitance matrix, C_p, is formed from the piezoelectric properties only. It is not a function of the structure properties for this case.

Ψ_r is the matrix of assumed shape functions for beam displacement. Since the Rayleigh-Ritz method was used, the only requirement for this complete set of basis functions is that each function obey the boundary conditions of the geometry. The mass and stiffness matrices calculations also require the displacement shape functions be twice differentiable with respect to the generalized displacement coordinate, r. The displacement functions used for this structure are the first four mode shapes for a cantilevered beam. In practice higher modes of vibration in structures do not contribute much to the overall motion, and three modes are often adequate to describe the longitudinal vibration in a cantilevered beam (Inman, 1989). For this reason structures can be thought of as low pass filters. The derivation of the mode shapes for a cantilevered beam is shown in Appendix B, and these results are confirmed by Blevins (1979). The fundamental assumption of modal analysis is that overall displacement and potential functions, described below, can be expressed as an infinite sum of the product of shape functions and time functions.

$$u(x,t) = \sum_{n=1}^{\infty} r(t)\Psi_r(x) \quad \text{and} \quad \varphi(x,t) = \sum_{n=1}^{\infty} v(t)\Psi_v(x)$$

Another way of saying this is that the overall displacement and potential solutions are separable in space and time. Since higher modes of vibration do not contribute much to

the overall motion, four modes will be retained for this model.

Assumed shape functions for the potential field in the piezoelectrics were used to derive the expressions for the capacitance, C_p, and coupling, Θ, matrices. These functions are linear in opposite directions with respect to distance through the thickness of the piezoelectric pair (Hagood, Chung and von Flotow, 1990).

$$\Psi_v = \begin{cases} 0 & x < a_{i1} \\ \dfrac{y - \frac{1}{2}t_s}{t_p} & a_{i1} < x < a_{i2} \ , \ y > \frac{1}{2}t_s \\ 0 & x > a_{i2} \\ 0 & x < a_{i1} \\ \dfrac{-y - \frac{1}{2}t_s}{t_p} & a_{i1} < x < a_{i2} \ , \ y < \frac{1}{2}t_s \\ 0 & x > a_{i2} \end{cases}$$

where a_{i1} and a_{i2} are the endpoints, in the x-direction, of the i^{th} piezoelectric ($a_{i1} < a_{i2}$), and y is measured from the center of the beam perpendicular to its longitudinal axis (see the coordinate system and origin in Fig. 3.1).

Electrical circuit equations were found using KCL at nodes A and B (see Fig. 3.1) using the non-ideal op-amp model discussed earlier.

$$\text{node A:} \quad \dot{q}_2 = -R_i^{-1} v_2 + R_f^{-1}(v - v_2) + C_f \frac{d(v - v_2)}{dt}$$

$$\text{node B:} \quad \dot{q} = R_f^{-1}(v_2 - v) + C_f \frac{d(v_2 - v)}{dt} - R_o^{-1}(v + kv_2)$$

where k is the op-amp open-loop gain. Remember that the time derivative of charge is current; $\dot{q} = i$. An ideal model was used to represent the electrical transformer. The constitutive equations for it are $Nv = v_1$ and $N\dot{q}_1 = \dot{q}$, where N is the transformer turns ratio. Special attention should be paid to the current directions and voltage references used here. Note that $\dot{q}$ is the positive current that flows into the transformer from the op-amp side, and $\dot{q}_1$ is the positive current that flows from the transformer to the piezoelectrics. Substituting the transformer equations along with the sensor equation above, the electronics equations become:

$$\Theta_2{}^T\dot{r} + C_{p2}\dot{v}_2 + R_i^{-1}v_2 + R_f^{-1}(v_2 - \frac{1}{N}v_1) + C_f(\dot{v}_2 - \frac{1}{N}\dot{v}_1) = 0$$

$$N(\Theta_1{}^T\dot{r} + C_{p1}\dot{v}_1) + R_o^{-1}(kv_2 + \frac{1}{N}v_1) + R_f^{-1}(\frac{1}{N}v_1 - v_2) + C_f(\frac{1}{N}\dot{v}_1 - \dot{v}_2) = 0$$

where Θ_1 and Θ_2 are columns one and two of Θ respectively, and C_{p1} and C_{p2} are elements 1,1 and 2,2 of C_p respectively. Note that C_p is a diagonal matrix in this case, so the charge and voltage are uncoupled and act independently. Therefore, the charge of each piezoelectric is a function of its voltage and the modal displacements. These equations can be manipulated into the form:

$$\dot{v}_1 = A_{r1}\dot{r} + A_{v11}v_1 + A_{v21}v_2$$

$$\dot{v}_2 = A_{r2}\dot{r} + A_{v12}v_1 + A_{v22}v_2$$

Now, a closed-loop state representation can be formulated for the entire BPE system using the actuator equation:

$$\dot{X} = A \cdot X$$

$$\begin{bmatrix} \dot{r} \\ \ddot{r} \\ \dot{v}_1 \\ \dot{v}_2 \end{bmatrix} = \begin{bmatrix} 0_{nxn} & I_{nxn} & 0_{nx1} & 0_{nx1} \\ -M^{-1}K & -M^{-1}C & M^{-1}\Theta_1 & M^{-1}\Theta_2 \\ 0_{1xn} & A_{r1} & A_{v11} & A_{v12} \\ 0_{1xn} & A_{r2} & A_{v21} & A_{v22} \end{bmatrix} \begin{bmatrix} r \\ \dot{r} \\ v_1 \\ v_2 \end{bmatrix}$$

The addition of the feedback circuit adds two states, v_1 and v_2, to the original eighth order piezostructure. The solution of this matrix equation is $X(t) = X(t_0) \cdot e^{At}$, which was carried out numerically (in `BEAM2.M`).

3.2.2 BPE System Power and Energy

Upon solving the closed-loop system matrix equation, the response of all the state variables to the initial conditions $X(t_0)$ was found. From the piezoelectric voltages, all the power variables (effort and flow), and therefore energy, can be found at every port in the circuit. Analogous to the single degree-of-freedom systems, the expressions for reactive energy in a flexible multi-degree of freedom, mechanical system described by differential equations in the form of the actuator equation are:

$$\text{Kinetic Energy} = T = \tfrac{1}{2}\dot{r}^T M \dot{r} \qquad \text{reference 11}$$

$$\text{Potential Energy} = V = \tfrac{1}{2} r^T K r$$

The expression for power dissipation in a mechanical system described in terms of ordinary differential equations is:

$$\text{Dissipated Power} = U = \dot{r}^T \mathfrak{D} \dot{r}$$

This comes from the fact that the effort, or force in this case, due to damping in each

mode in the structure, $\mathfrak{D}\dot{r}$, is multiplied by the flow or velocity of each mode. This expression is verified using the open-loop piezostructure simulation. The only dissipation mechanism in the open-loop system is damping. For energy investigation purposes in this thesis, the power dissipation expression is integrated numerically using Simpson's $\frac{1}{3}^{rd}$ rule.

The sourcing and sinking (dissipation) of energy in the op-amp is most important to this research since the op-amp is the only power supplying component in the system, and amplification is the most common form of signal processing (Franco, 1988). All other power flow in the system is either dissipative or reactive. Since primitives used may differ from model to model, the op-amp model affects the power flow, but accurate models should result in the same net energy transfer.

The BPE system power flow will be simulated using two different op-amp models. In addition to the op-amp model in Fig. 3.4, a new model was investigated because the source in the Fig. 3.4 model does not maintain a constant effort. The model considered here is a black box model because the internal transistors, etc. are not modeled directly with other primitives, and a boundary is drawn around the op-amp across which only power flowing into and out of the op-amp is considered. Figure 3.5 shows the constant effort source model. A possible problem with this model is that it does not show specifically where power is dissipated in the op-amp. Dissipation in the resistors and transistors in the real op-amp is not specifically represented. All power is assumed to be absorbed into the low voltage rail. It would be very difficult to use a model that employs all the resistors and transistors in a real op-amp.

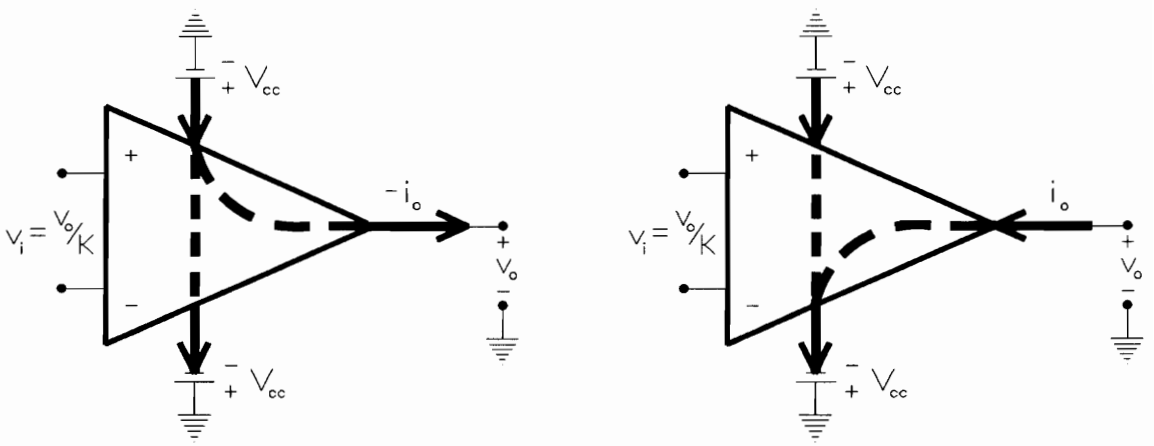

Figure 3.5: Constant Source Op-Amp Model: (a) Sourcing and (b) Sinking Current

This model uses the standard op-amp assumption that no power flows into the input terminals. Therefore, power can only flow through the output terminal and the supply rails. The output voltage must be in the range $\pm V_{cc}$ because the internal transistors saturate if the output is out of this range. Therefore, $+V_{cc}$ is the most positive voltage in the circuit, and current always flows from this source, and since $-V_{cc}$ is the most negative, current always flows into this source. Current may flow into or out of the output terminal of the op-amp depending on the circuit conditions (i.e. voltages). Therefore, the op-amp may source or sink current, and since the rail voltages are constant, the op-amp may source or sink power. Figure 3.5a shows the case of the op-amp sourcing current, and Fig. 3.5b shows the case of the op-amp sinking current. In the cases investigated in this work, the object is to decrease the natural settling time of an initially energetic, mechanical system. Therefore, the average power flow must be from beam to electronics.

The calculation of the power flow in the second model is straightforward. Regardless of the output current properties, the current needed to bias the internal transistors and diodes that make up the op-amp is constant for a given op-amp. Typically this quiescent supply current is in the mA range. For the 741 op-amp used here I_q = 1.7 mA (Franco, 1988). In newer, more expensive op-amps, the quiescent supply current is in the μA range, and power flow is often negligible. This current experiences a voltage drop of V_{cc} - (-V_{cc}) or $2V_{cc}$. When a flow variable experiences an effort drop, the power is, P = (effort drop) · flow, and this power is always dissipated in the op-amp. As noted before, the op-amp can either source or sink power depending on the output current direction. The sign of i would be changed to negative in the case of the op-amp sinking current as in Fig. 3.5a. Therefore, total op-amp power would be:

$$P_{op\text{-}amp} = 2V_{cc}I_q + (V_{cc}|i| - v \cdot i)$$

where i and v are the current and voltage at the op-amp's output terminal. Note that the signs of i and v depend on external circuit conditions, and these signs determine whether power flows into or out of the op-amp. The sign convention assumed with this op-amp model is that v is positive at the op-amp output terminal if referenced to ground, and i is positive when it flows out of the op-amp as in Fig. 3.5b.

Now energy can be completely quantified and investigated in the BPE system using each op-amp model. The theory above has been encoded into MATLAB's programming language. The second m-file in Appendix C, `BEAM1.M`, calculates the BPE system matrices - mass, stiffness, electro-mechanical coupling, and capacitance. The third m-file,

BEAM2.M, solves for the state variables due to initial conditions of the closed-loop BPE system. The fourth, BEAM3.M, calculates and displays power flow and energy transfer in the system according to the variable source op-amp model, while the final m-file, BEAM4.M, calculates and displays power flow and energy transfer in the system according to the constant source op-amp model.

Chapter 4

Simulation Results

4.1 Simple Systems

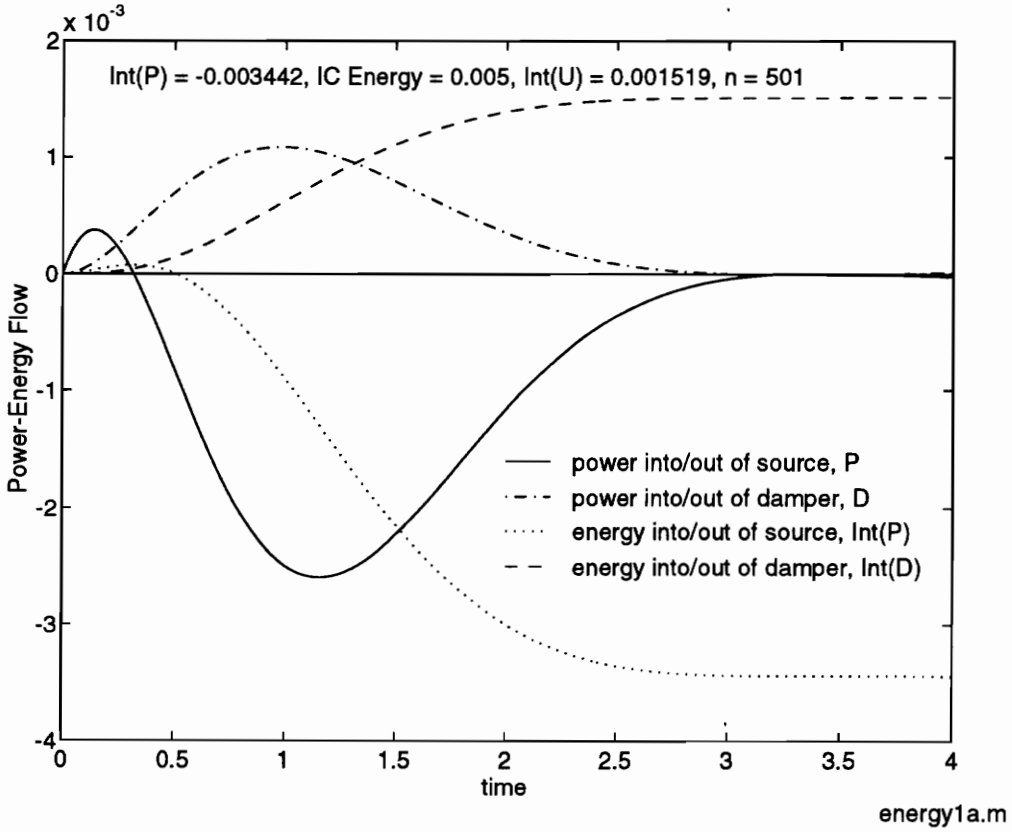

Figure 4.1: Power/Energy Initial Condition Response of SMD System

Figure 4.1 is a plot of the power-energy response of the controlled SMD system due to initial conditions. The response is a result of running `ENERGY1A.M`, shown in Appendix C, with the following conditions:

initial conditions: displacement: 0.1 m; velocity: 0 m/s

spring stiffness: 1 N/m

damping ratio: 0.15

mass: 1 kg

control law: full state feedback via LQR with equal weight on states and input

The initial conservative (potential and kinetic) energy in the system exits through the damper, of course, and less obviously through the ideal source (force). Since energy is the integral of power, the energy exiting the system over a certain interval of time can be calculated using any of a number of numerical integration schemes. According to conservation of energy, the energy exiting the system over the transient period up to steady-state, zero-displacement and zero-velocity, should balance the initial energy in the system. Since this SMD system has reached steady-state in about four seconds, the integral of the damper power curve from zero seconds to four seconds plus the integral of the source power curve from zero seconds to four seconds should balance the initial energy of 0.005 J due to the initial spring extension. The non-dissipating primitives present in this system are the mass (inertial primitive) and the spring (capacitive primitive). The initial energy is calculated by evaluating their energy expressions at the initial conditions of the system. According to the sign convention discussed earlier, positive damper power, and therefore

energy over a time period, means power into the damper or out of the system, and negative source power means power into the source or out of the system. Summing the absolute values of the source and damper energy results an energy dissipation value of 0.0050 J to two significant figures. This balances the initial energy in the system.

The number of significant figures can be increased by increasing the number of integration steps. Figure 4.1 shows that these power curves are very smooth, that is, the frequency of vibration is such that a small number of oscillations occur in the transient period. Numerical integration is more efficiently performed when this is the case. The number of points defining the integrand must be increased to account for roughness in the integrand. Even though the curves used in this simple example were rather smooth, 501 points were required to achieve good integration results over four seconds. Realistic systems result in rough power curves with higher frequency of oscillation and therefore more points are required to define the integrand.

If there were no damping in the system, then all of the initial energy would have to be transferred out or displaced by the input source. Figure 4.2 shows the power and energy curves for this case with the same initial conditions. The simulation shows that the power and energy curves have the same general shape as the case where damping was present except that all the initial energy is dissipated by the source. The trend is that as the damping coefficient is increased, energy dissipated by the damper increases asymptotically. Figure 4.3 shows the energy dissipation in the spring-mass system as a function of damping ratio, ζ. The damping ratio is usually used to specify damping in a mechanical,

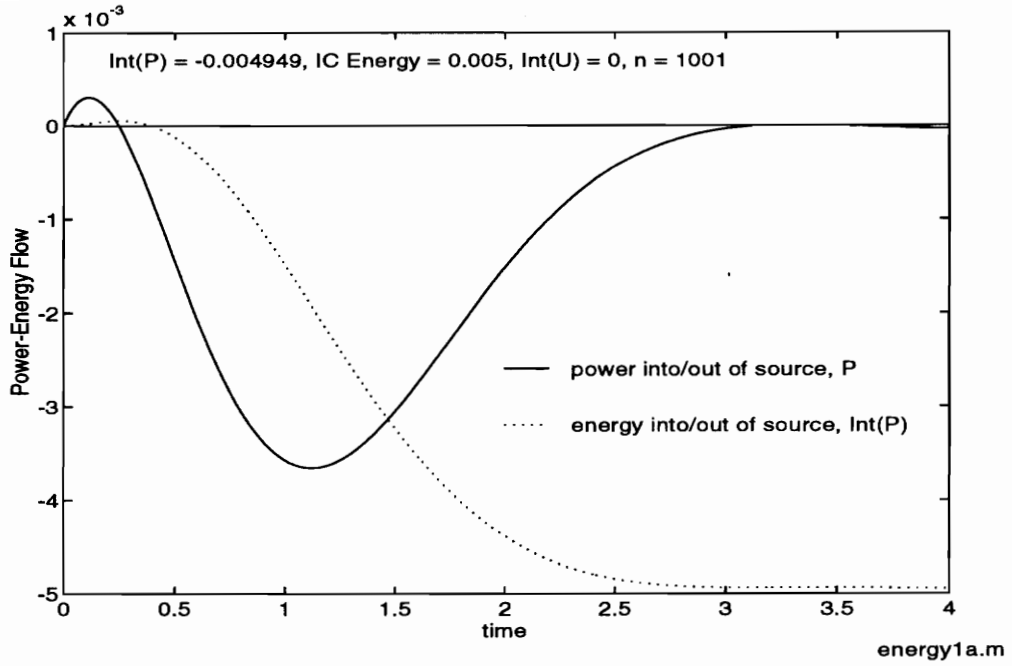

Figure 4.2: SMD Power/Energy Initial Condition Response With No Damping

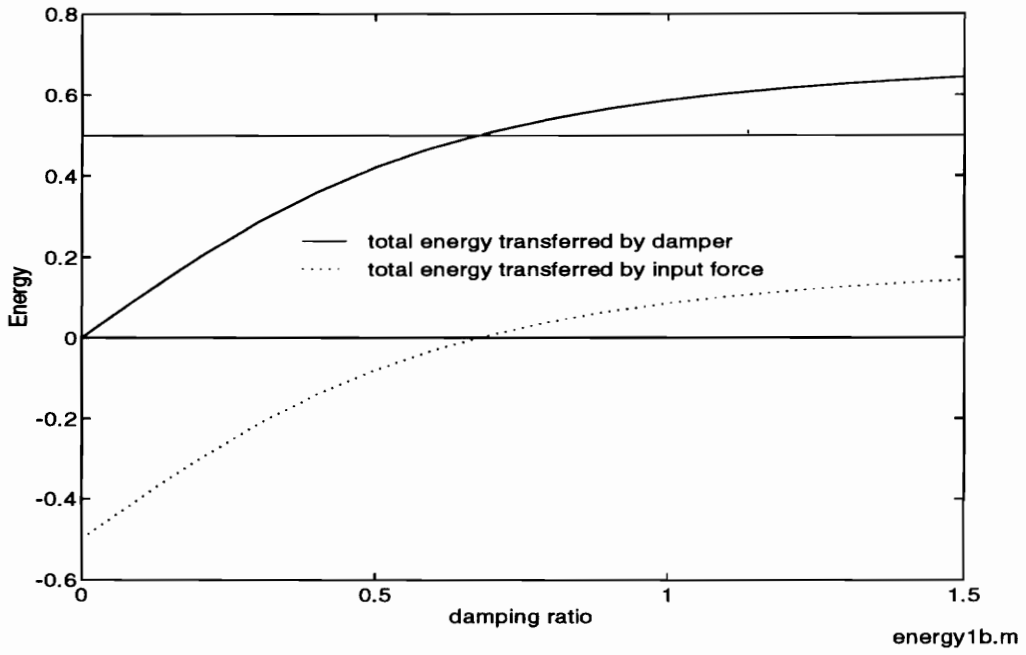

Figure 4.3: Energy as a Function of Damping Ratio for the SMD System

vibrating system because it can be determined experimentally from the free vibration data of the system (James, et al., 1989), while the damping coefficient, c, usually cannot. The damping ratio is dependent on system parameters, such as mass, stiffness and geometry. Since the only dissipating devices in the system are the damper and the source, the curves have the same shape. The difference between them at any damping ratio value is the initial energy in the system. Note that as damping ratio increases, there is a point ($\zeta \approx 0.7$) where the force begins to add energy to the system because the control design requires a response that is faster than possible with the inherent damping.

This all seems to be elementary because as noted before, energy is always conserved, but energy transfer becomes somewhat ambiguous if we look at where the energy goes. Power always flows out of the system into the damper, and this is intuitively true since a damper is a resistive element, but according to the simulation, power flows into and out of the source also. A source is thought of as supplying power, which accounts for the sign convention, but in order for the initial energy to leave the system, some must exit through the source. Figure 4.4 shows that power flows into and out of the source. Since power flows into this source during the first 0.33 seconds and out during part of the time response, the source could be approximated by some combination of a capacitive primitive and a resistive primitive. Remember that a capacitive primitive is power conserving; that is, power that flows into the primitive must eventually flow out. Figure 4.4 shows that more energy must flow out through the source than flows in from it. Therefore, a resistive primitive must accompany the capacitive primitive in making up the source. If Fig. 4.1 is

again considered, it is noted that power initially flows out of the source. These response results differ from those shown in Fig. 4.4 because the initial conditions have been changed to: displacement: -1 m, velocity: -0.5 m/s. All other simulation conditions are the same. The results of Fig. 4.1 suggest that, in order to satisfy the power flow requirements of the controller in combination with these initial conditions, a power source must initially be present. Therefore, to handle a variety of initial conditions, the overall source could contain a capacitor, a resistor and a power source. The advantage of the overall

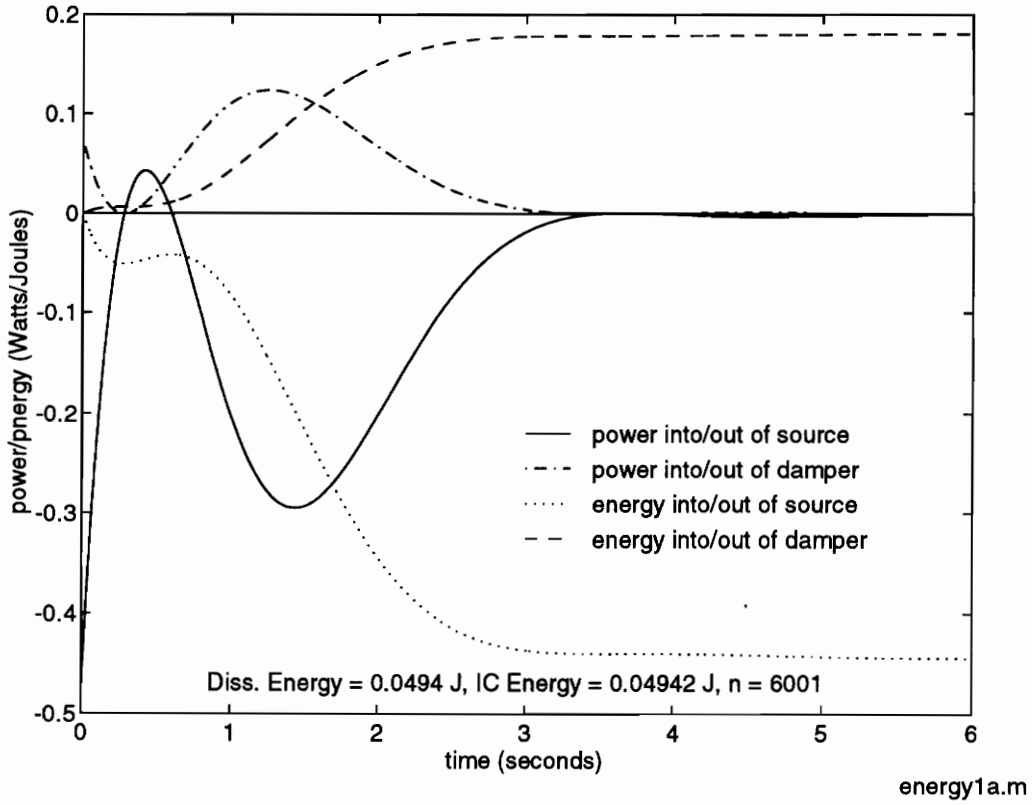

Figure 4.4: SMD Power/Energy Initial Condition Response

source containing a capacitive primitive is that less power is required from the power source. Energy that is stored in the capacitor can be used as if it comes from the power source. The more the capacitive primitive is used the less energy is dissipated into the source and resistor.

The control force used here is imaginary; an actual forcing actuator has not been modeled. A physically realizable actuator would likely contain a voltage source, e.g., an electrical outlet. It is difficult to imagine how power is dissipated or absorbed into an electrical source. How can power flow into the outlet be realistically modeled, and what are the effects of this flow? The simulation of this simple system shows that power must flow into the source in order to allow the controller to work as designed, but this system is not very complex or realistic. In the following sections, the results of power flow and energy transfer in a physically realizable system are presented with the hope that energy transferred into the source can be stored and used when needed instead of being lost.

4.2 Beam-Piezoelectrics-Electronics (BPE) System

4.2.1 BPE System Open-Loop Characteristics

First, the piezostructure response was simulated to understand dissipation of energy due to damping in distributed parameter systems approximated by ordinary differential equations. All the energy dissipation in the piezostructure is accounted for through

damping because no other dissipative primitives are connected to the system through the piezoelectrics' electrodes. Since the final state of the piezostructure is a no-energy state, no motion and no stored energy, the initial conservative energy in the system should match the dissipated energy at the final state. Figure 4.5 shows that the initial energy in the system, 0.04942 J, due to an initial tip displacement of 5 cm. on the beam, leaves the system by virtue of the damping distributed throughout the beam's volume. Initially, the beam is specified to assume the first mode shape with the tip displacement given above. The results of this open-loop simulation prove that the expression for damping dissipation given in section 3.2.2 ($U = \dot{r}^T \mathcal{D} \dot{r}$) is valid.

Figure 4.6 shows that the frequency of oscillation of the damper power curve is about 30 Hz. Consequently, a large number of points must be used to specify this power curve for integration purposes when the integration interval is four seconds. Since this number must be large, long computer run times are inevitable. Modeling accuracy is affected by the number of points used to specify mode shape values along the beam length. This value affects the accuracy of the model representing the piezostructure because, as mentioned before, it is used in the integration calculation of the system matrices. In both cases, the greater the number of points specifying a vector of numbers to be integrated numerically, the better the accuracy of the calculated dissipated energy of the piezostructure due to damping. Along the piezostructure length, 200 steps were used to approximate the distributed parameter system, and 6000 time steps were required to achieve two significant digits of energy accuracy. When compared to the power curves for the simple

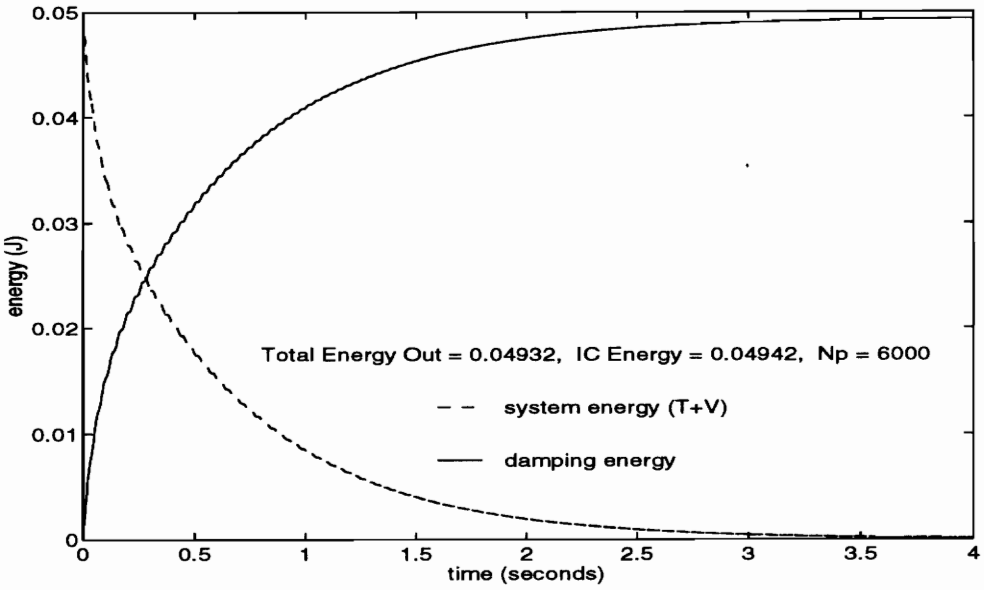

Figure 4.5: Energy Transfer In The Open-Loop BPE System

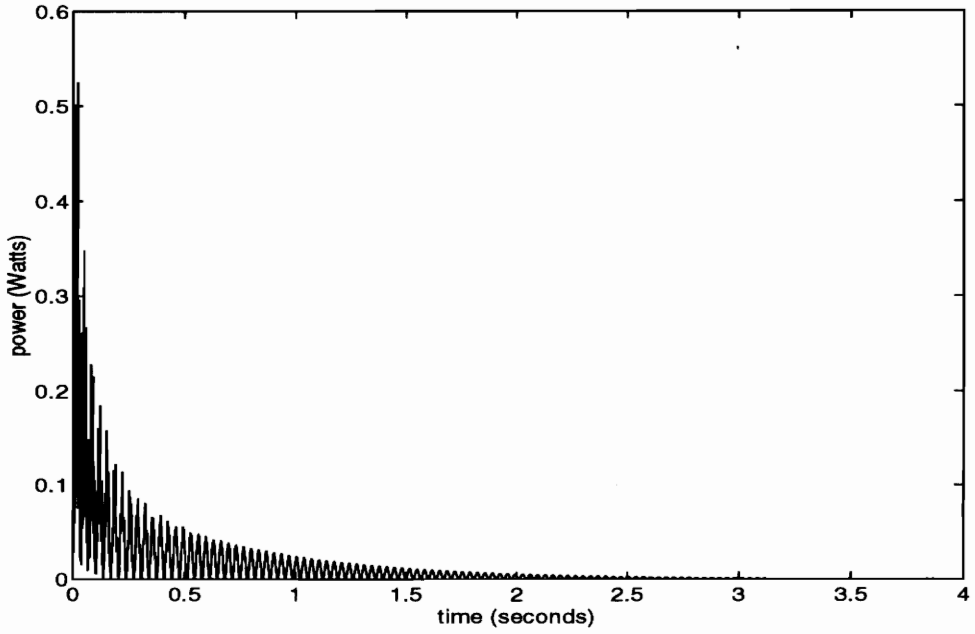

Figure 4.6: Power Flow In The Open-Loop BPE System

systems, it is obvious that numerical errors are more difficult to overcome in the BPE system.

After considering the piezostructure alone, it is desirable now to see what control the output feedback law will have on the beam's motion. The root locus plots of the transfer function between the system output (v) and the system input (v_1) for the piezostructure with op-amp circuit (Fig. 3.1) are plotted in Fig. 4.7 and Fig. 4.8. The properties used for electrical components in the feedback circuit are tabulated in Table 4.1.

Table 4.1: BPE System Electronic Properties

Feedback Capacitor	C_f	$1 \cdot 10^{-6}$ Farads
Feedback Resistance	R_f	100 kΩ
Op-amp Gain	k	200000
Op-amp Input Resistance	R_i	2 MΩ
Op-amp Output Resistance	R_o	75 Ω

The SSE for the open-loop system is

$$\begin{bmatrix} \ddot{r} \\ \dot{r} \end{bmatrix} = A_o \begin{bmatrix} \dot{r} \\ r \end{bmatrix} + B_o v_1 \quad \text{and} \quad v = C_o \begin{bmatrix} \dot{r} \\ r \end{bmatrix} + [0] v_1 .$$

A_o, B_o, C_o and D_o are calculated using the actuator and sensor equations and the KCL circuit equations. The results are given in `BEAM2O.M` (see Appendix C). The open-loop eigenvalues or complex pole pairs are:

$-38.68 \pm 3850i \quad \Rightarrow$ fourth mode pair
$-20.00 \pm 1995i \quad \Rightarrow$ third mode pair
$-7.110 \pm 715.6i \quad \Rightarrow$ second mode pair
$-0.7368 \pm 92.19i \quad \Rightarrow$ first mode pair

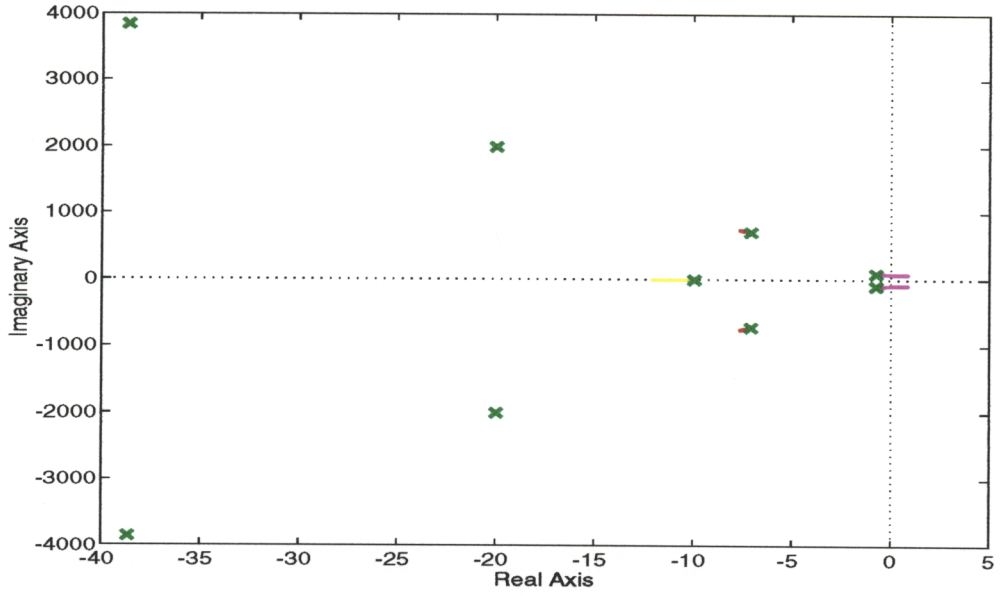

Figure 4.7: Root Locus for $V(s)/V_1(s)$ For Positive Gain (N)

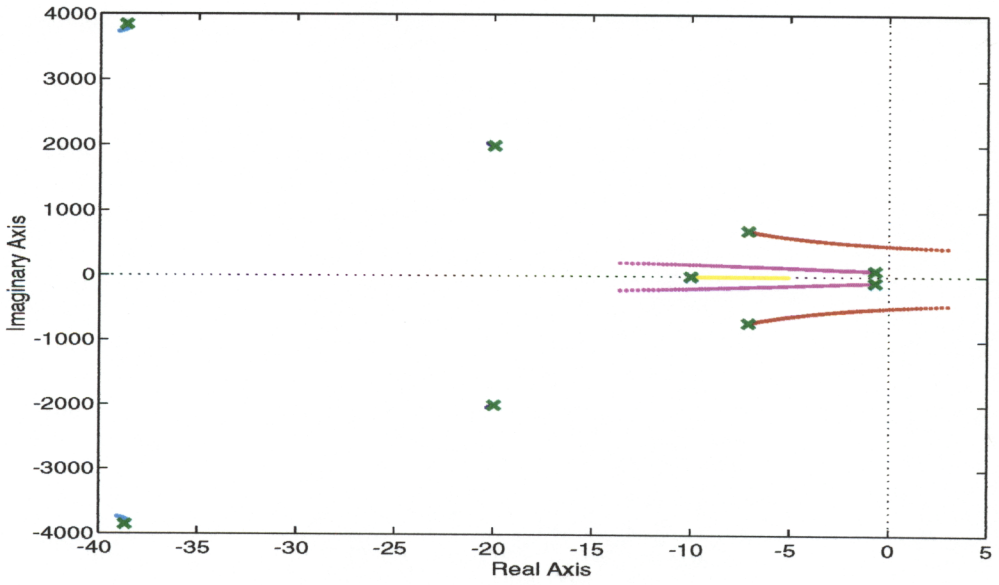

Figure 4.8: Root Locus for $V(s)/V_1(s)$ For Negative Gain (N)

The four pairs of complex poles represent the four retained modes used to calculate system parameters like mass and stiffness for the piezostructure. The magnitude of these root locations is the undamped natural frequency of the corresponding mode. The four undamped natural frequencies can be obtained by finding the magnitude of the eigenvalues of A_o. They are

$$f_n = 14.67, 113.9, 317.5 \text{ and } 612.7 \text{ Hz.}$$

Since damping is present in the system, the frequency at which the structure will resonate, the damped natural frequency, is slightly decreased. In real structures, the damping ratio is usually small ($\zeta < 0.1$), and therefore, the resonant frequency is usually approximated by the undamped natural frequency (James et al., 1989). Damping in the piezostructure is assumed to be very small. The modal damping ratio used here, $\zeta_n = 0.01$, was found by matching the free response to initial conditions of a test piezostructure to the simulation.

Figure 4.7 shows that a positive gain between v and v_1, the output feedback gain, should not be large. The roots due to the dominant first piezostructure mode move toward the right into the unstable plane as the gain is increased while the roots due to the second mode move only slightly left. The third and fourth mode root pairs do not move noticeably. At an output feedback gain of about 25, the system begins to go unstable, and at this gain the other roots have moved only slightly left. Therefore, the system performance in the form of settling time can not be improved significantly with a positive gain.

To get better first mode performance, the feedback gain must be negative. Figure 4.8 shows the root locus for this case. The roots due to the second piezostructure mode

move toward the left as the gain is decreased while the roots due to the dominant first mode move left. At an output feedback gain of about -249, the system begins to go unstable due to the right half plane movement of the second mode poles, and at this gain the first mode poles have moved left. The first mode is dominant in the system because the contribution to the beam motion from the other modes decays much faster. This is obvious when looking at the next figure. Figure 4.9 shows the open-loop modal displacement response of the piezostructure to initial conditions.

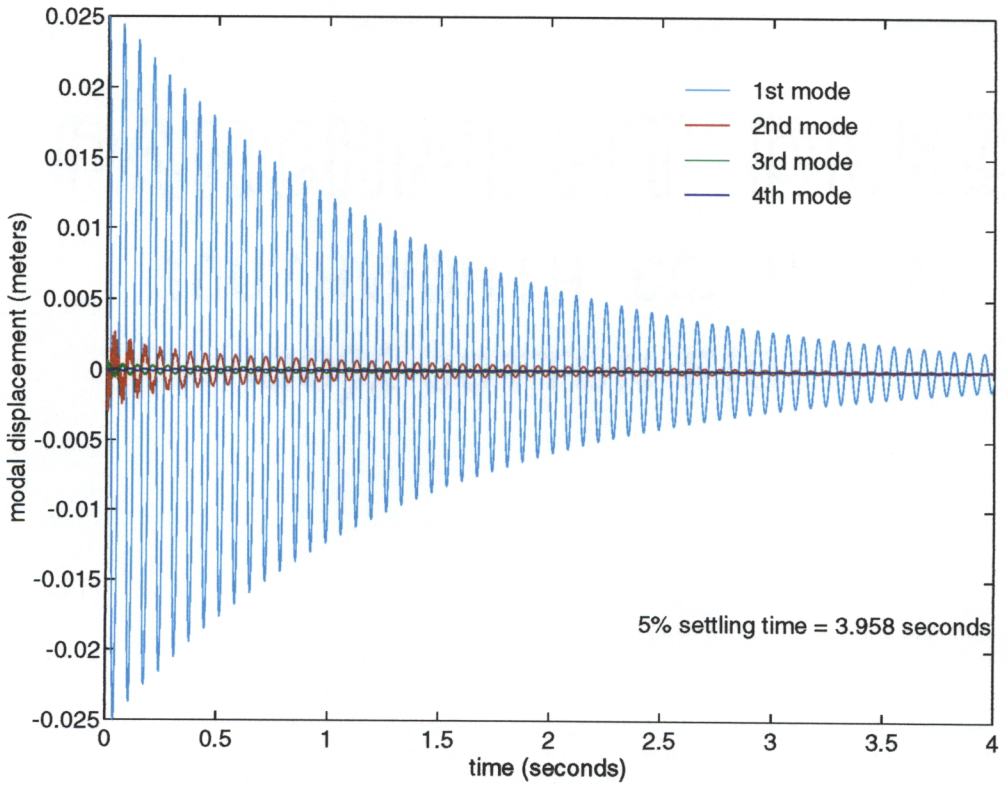

Figure 4.9: Open-Loop Modal Displacement Response of the Piezostructure to IC's

The system matrices, A, B, C and D, are fully populated; and therefore, the modes used here are coupled. This comes from the method reviewed in section 3.2.1 of this thesis, in which the actuator and sensor equations for the piezostructure are calculated. The fact that they are coupled means that the displacement of the first mode is affected by the displacements and velocities of the other modes. Uncoupled modal displacements can be found using some transformation matrix. The purpose of viewing the modal displacements is to find settling times and compare to closed-loop systems, so uncoupling is unnecessary.

Physical implementation of a negative feedback gain involves reversing the polarity of one of the transformer voltages, v or v_1. The closed-loop simulations were performed with a gain, or transformer turns ratio, of $N = -5$. The eigenvalues, or poles, of the closed-loop state matrix for this value of N and the electrical properties listed in Table 4.1 are listed below.

$-1.642 \cdot 10^9$
$-38.67 \pm 3847i \Rightarrow$ fourth mode pair
$-20.01 \pm 1995i \Rightarrow$ third mode pair
$-7.050 \pm 711.9i \Rightarrow$ second mode pair
$-8.808 \pm 93.45i \Rightarrow$ first mode pair
-9.830

As shown in chapter 3, the addition of the feedback circuit has added two states to the system, resulting in two added poles. Note that the third and fourth mode pairs have not moved when compared to the open-loop poles, while the second pair has moved slightly right. The dominant first mode poles have moved farther left than any other poles.

4.2.2 BPE System Closed-Loop Characteristics

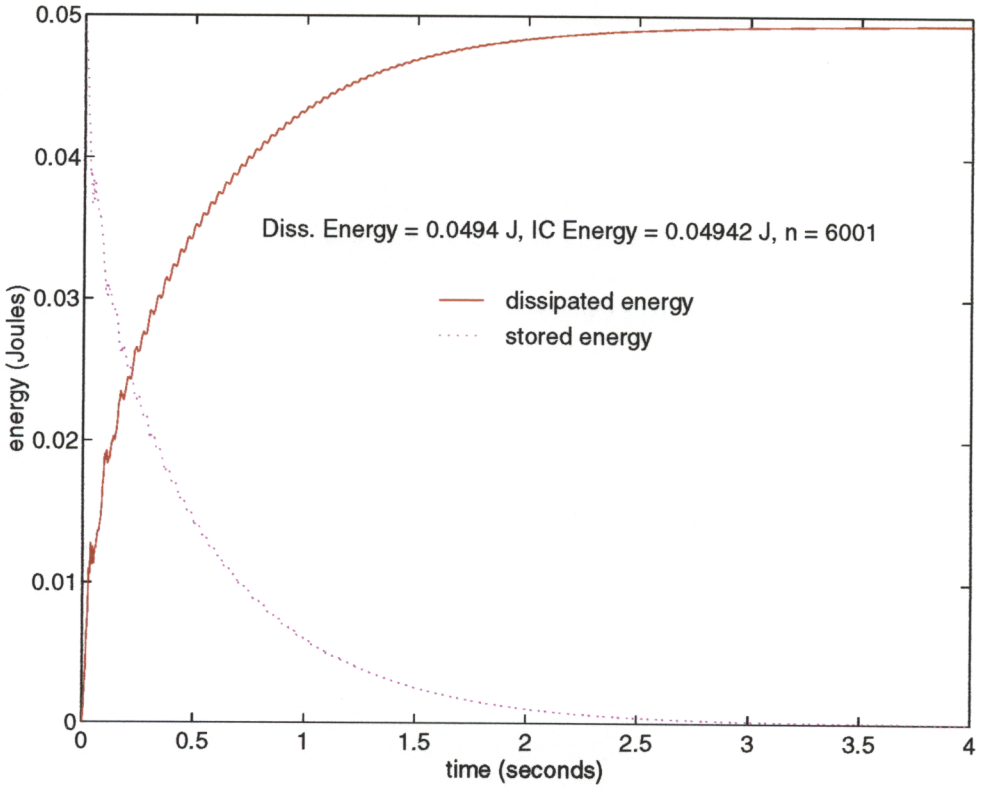

Figure 4.10: Total Energy Transfer in the Closed-Loop BPE System

Figure 4.10 shows how energy is dissipated as a function of time in the BPE system when the loop is closed between the two piezoelectric pair voltages through the op-amp circuit. The dashed line represents the conservative (kinetic and potential) energy sum, while the solid line represents the total energy entering and exiting the system. Energy leaves the system through viscous damping in the piezostructure and electrical resis-

tors in the feedback path. Notice that the curves are almost perfect mirror images of each other, supporting the power and energy calculations.

The purpose of Fig. 4.11 is to show that the closed-loop response improved when

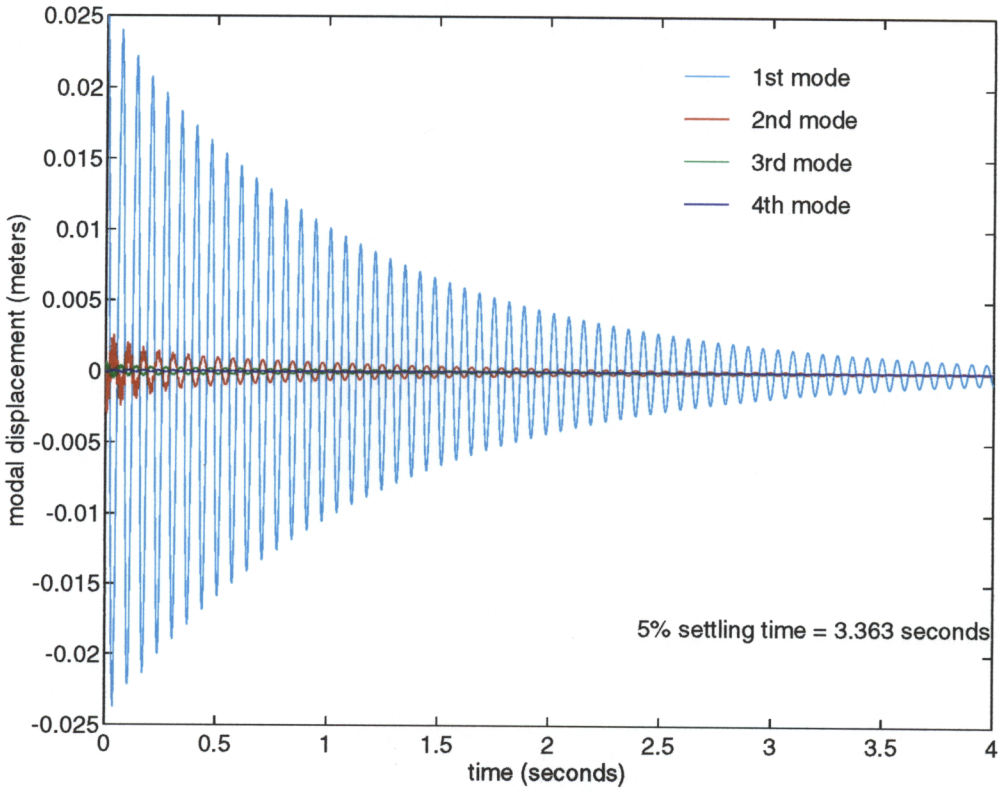

Figure 4.11: Closed-Loop Modal Displacement Response of the Piezostructure to IC's

compared to the open-loop response. It shows the closed-loop (coupled) modal displacement response. As expected, the first mode is the last to go to steady-state. The other modal displacement shapes reach steady-state long before the first mode does. The 5% settling time for the dominant first mode for the open-loop piezostructure shown in

Fig. 4.9 is 3.958 seconds , while the closed-loop settling time is improved to 3.363 seconds, a 16% decrease. The following figures show the power/energy curves for some important primitives in the BPE system.

Using the op-amp model from Fig. 3.4, the power and energy curves for the internal power supply is shown in Fig. 4.12. The simulation shows that power is absorbed into this source, while over the entire transient range, energy is transferred from the source to the rest of the system. Figure 4.13 shows the op-amp output resistance power/energy response. The power dissipated by the op-amp input resistance was found to be negligible. Note that the final energy values in Fig. 12 and Fig. 13 show that overall, energy is transferred from the beam to the op-amp. It is important to also know the overall power dissipation of the op-amp. This is simply the sum of the power dissipation in the input and output resistors minus the source power.

Like electrical capacitors, piezoelectric materials can only withstand a certain voltage. For the piezoelectric material considered here, this maximum voltage is 2 to 3 volts per 0.001 in. thickness (Piezotronics Division of AIM Technologies, Inc.). The maximum voltage applied across the electrodes of the actuating pair in the simulation was found to be about 80 volts. Recalling that this pair contains two 0.020 in. thick patches, the maximum voltage that should be applied across this pair is 80 volts. For larger tip displacements or different initial conditions and larger control gains (N), the resulting pair #2 voltage could be larger than the maximum rated voltage. An effort has been made here to keep this simulation realistic so that future experimental work can be done to verify the

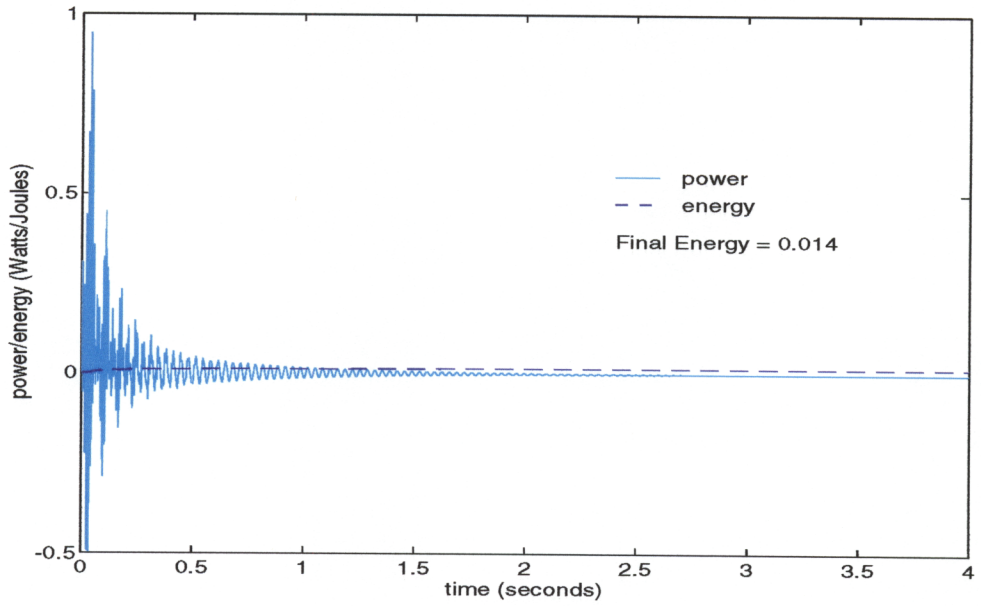

Figure 4.12: Power/Energy Response of the Op-Amp Internal Source

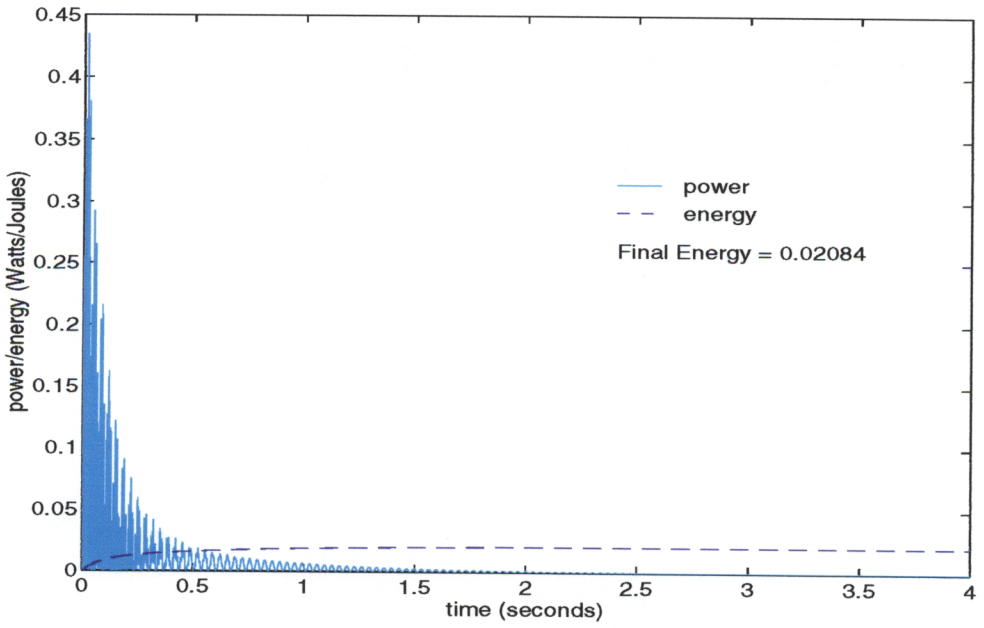

Figure 4.13: Power/Energy Response of the Op-amp Output Resistor

concepts introduced here. Of course the control voltage applied across the actuating piezoelectric pair is a function of the initial conditions and the amount of control desired.

Figure 4.14 shows the overall op-amp power dissipation as a function of time for the first two seconds of the response. The maximum power dissipated is about 0.83 watts. The data sheets for the 741 op-amp used here give a maximum power dissipation of 0.57 watts (Franco, 1988). The op-amp power dissipation should not be more than that specified by the manufacturer. Note though that most of the time, the power being dissipated by the op-amp is less than 0.57 watts. Newer, more expensive op-amps are capable of dissipating much more than a watt. This plot is very significant because it shows characteristics of a capacitive component. This suggests that in place of the source used to power the op-amp a capacitive primitive can be used. Energy is conserved in an ideal capacitor; it stores and gives up energy without loss. Therefore, the negative half of the power flow in Fig. 4.12 could ideally be stored as energy in a capacitor and given back to the system. The problem with this is that the control design may require a variable, controllable voltage. One possible solution is a capacitor with a variable capacitance. Since more energy is transferred out of the source, a power source must be used in conjunction with the capacitive primitive, but the amount of exterior power required to make the system act as designed could conceptually be decreased.

As a comparison, power flow in the BPE system was simulated using the model shown in Fig. 3.5 (`BEAM4.M` in Appendix C). Figure 4.15 shows the results. This power curve is very similar to the variable source power curve. Although the magnitude differs

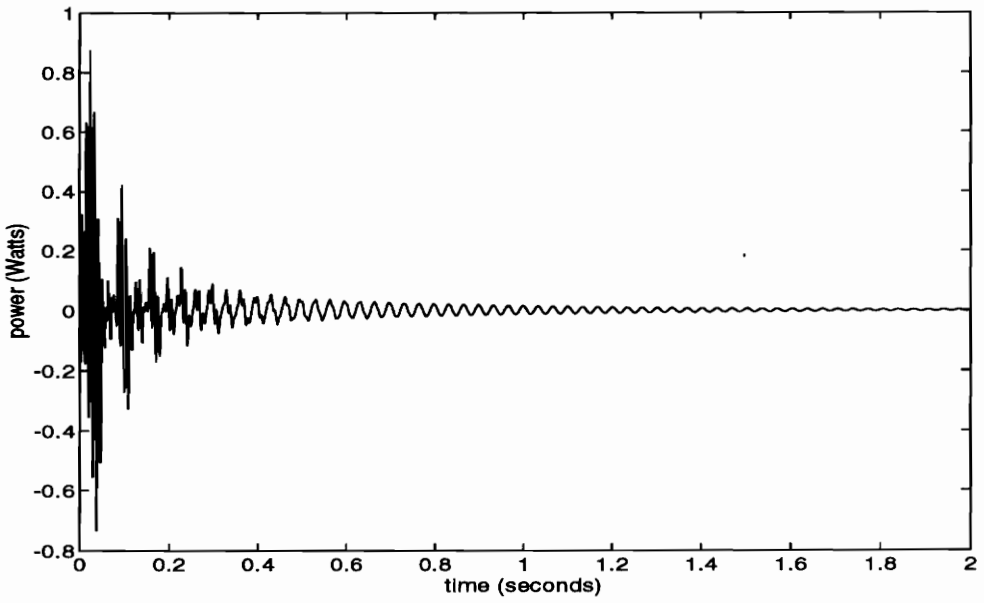

Figure 4.14: Total Op-Amp Power Response Using Variable Source Op-amp Model

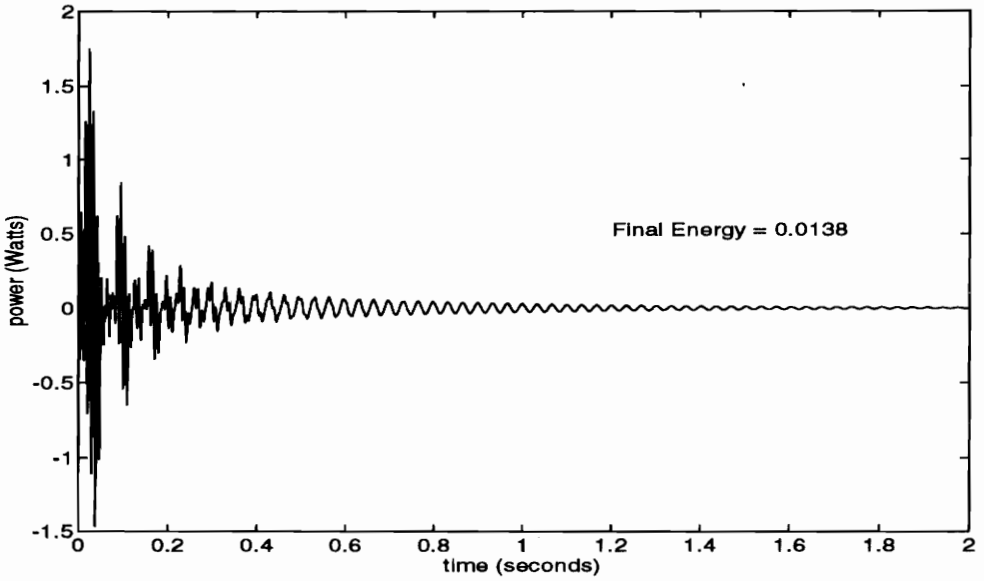

Figure 4.15: Total Op-Amp Power Response Using Constant Source Op-amp Model

between these two plots, the general shape is almost identical. This supports the claim that a capacitive primitive can be used with a source to minimize external power consumption. After closer inspection, the magnitudes seem to be closely related. The power dissipation calculated from the constant source model is always twice the dissipation due to the variable source model. The problem with the constant source model is that power flowing into the source and power sinking into transistors and resistors are not distinguishable.

Other miscellaneous things to note about the energy transfer in this system follow. The amount of energy dissipated through damping was reduced by a small amount because the feedback control loop slowed the modal velocities. The extra energy in the system due to less viscous damping in the beam was forced out mostly through the op-amp. The final energy lost through the op-amp feedback resistor was only $1.989 \cdot 10^{-4}$ J. The dissipation of energy in the op-amp input resistor was only on the order of 10^{-16} J. The supports the often used ideal op-amp assumption that no current flows into the input terminals.

Chapter 5

Conclusions and Recommendations

5.1 Conclusions

Power flow and energy transfer has been simulated for the simple spring-mass-damper system and the more complex and realistic beam-piezoelectric-electronics system. The SMD system simulations show most significantly that power seemingly flows into power supplies that make up the controller. It was suggested in the case of an electrical power source, as in the BPE system case, that an electrical capacitor could be used in conjunction with a power source to store and supply energy and therefore minimize the external power needed to make the controlled system function as desired.

This research began with the hopes that energy could be put back into the source for the reasons discussed above. The problem with physically implementing the concepts presented here is that the model may not accurately represent the source primitives in the actual component. Two op-amp models were used in the simulations for the BPE system, and both models exhibited similar overall power flow characteristics. The question that still remains is: Does the energy actually flow into the source or is it dissipated in transis-

tors and resistors in the op-amp? Neither model gives a definite answer to this question. The variable source model suggests that energy does flow into the rails, which are represented by the variable source, and dissipation in the op-amp is through input and output resistances only. Using the constant source op-amp model it is not possible to distinguish between power dissipated through resistances and sources. In either case it is concluded that a simple source model may not be available for power flow analysis.

Regardless of whether power actually flows into control sources, this work served the purpose of accurately modeling and simulating energy transfer in a controlled piezostructure. Since vibration suppression requires removing energy from the vibrating system, this work is also considered a first step in creating control design methods based on energy transfer.

5.2 Recommendations

A reasonable next step in the research of this subject would be to conduct an experiment to measure power flow into and out of sources, e.g., in the BPE system, with the goal of designing a capacitive device that could function with a source to minimize power flow from an external source into the system. Investigation in this work refers to creating ideal system models and simulating them using MATLAB. An experiment could be done on the BPE system simulated because an effort was made to ensure that the model is as realistic as possible. Note that this work has only served to introduce a creative concept

that would require much experimental verification. In addition, the development of modified control approaches based on energy transfer could result from this initial study.

References

Bobrow, Leonard S. 1985. *Fundamentals of Electrical Engineering*. New York: Holt, Rinehart and Winston, Inc.

Blevins, Robert D. 1979. *Formulas for Natural Frequency and Mode Shape*. New York: Van Nostrand Reinhold Company.

Chapra, Steven C. and Raymond P. Canale. 1988. *Numerical Methods for Engineers*. 2nd ed. New York: McGraw Hill.

Cook, Robert D. 1981. *Concepts and Applications of Finite Element Analysis*. New York: John Wiley and Sons.

Crandall, Stephen H., Dean C. Karnopp, Edward F. Kurtz, Jr. and David C. Pridmore-Brown. 1968. *Dynamics of Mechanical and Electromechanical Systems*. Malabar, FL: Robert E. Krieger Publishing Co.

DeCarlo, Raymond A. 1989. *Linear Systems*. Englewood Cliffs, NJ: Prentice Hall, Inc.

deSilva, Clarence W. 1989. *Control Sensors and Actuators*. Englewood Cliffs, NJ: Prentice Hall, Inc.

Franco, Sergio. 1988. *Design with Operational Amplifiers and Analog Integrated Circuits*. San Francisco, CA: McGraw-Hill, Inc.

Hagood, Nesbitt W., Walter H. Chung, Andreas von Flotow. 1990. "Modelling of piezoelectric Actuator Dynamics for Active Structural Control", AIAA-90-1087-CP.

Hoffman, E.J. 1977. *The Concept of Energy*. Ann Arbor, MI: Ann Arbor Science Publishers, Inc..

IEEE Std. 176-1978. 1978. " IEEE Standard on Piezoelectricity".

Inman, Daniel J. 1989. *Vibration With Control, Measurement, and Stability*. Englewood Cliffs, NJ: Prentice Hall.

James, M. L., Smith, G. M., Wolford, J. C., and Whaley, P. W., 1989, *Vibration of Mechanical and Structural Systems*. Harper and Row, Publishers, New York.

Karnopp, Dean and Ronald Rosenberg. 1975. *System Dynamics: A Unified Approach*. New York: John Wiley and Sons.

Kirby, G. C., Matic, P., and Lindner, D. K. "Optimal Actuator Size and Location Using Genetic Algorithms For Multivariable Control.

Liang, C., Sun, F. P., Rogers, C. A., 1994, "Coupled electro-mechanical analysis of piezoelectric ceramic actuator-driven systems - determination of the actuator power consumption and system energy transfer." *Journal of Intelligent Material Systems and Structures*, Vol. 5, No. 1, pp. 12-20.

Liang, C., Sun, F. P., Rogers, C. A., 1993, "An Investigation of the Energy Consumption and Conversion of Piezoelectric Actuators Integrated in Active Structures."

Meirovitch, Leonard. 1980. *Computational Methods In Structural Dynamics*. Rockville, MD: Alphen aan de Rijn.

Meirovitch, Leonard. 1970. *Methods Of Analytical Dynamics*. New York: McGraw-Hill Book Company.

Miller, D. F., and Shim, J. 1987, "Gradient-Based Combined Structural and Control Optimization." J. Guidance, Control and Dynamics, Vol. 10, No. 3, pp. 291-298.

Piezotronics Product Specification Sheets. 1994. Piezotronics Division of AIM Technologies, Inc., Flemington, NJ.

Schulz, G., and Heimbold, G. 1983, "Dislocated Actuator/Sensor Positioning and Feedback Design for Flexible Structures." J. Guidance, Control and Dynamics, Vol. 6, No. 5, pp. 361-367.

Warkentin, David J., Edward F. Crawley, "Power flow and amplifier design for piezoelectric actuators in intelligent structures." SPIE 1994 North American Conference on Smart Structures and Materials, Orlando, 13-18 February, 1994.

Yang, S. M., and Lee, Y. J. 1993, "Optimization of non-collocated sensor/actuator location and feedback gain in control systems." Smart Mater. Struct., Vol. 2, pp. 96-102.

Appendix A

Derivation of state-space model for a simple spring-mass-damper (SMD) system:

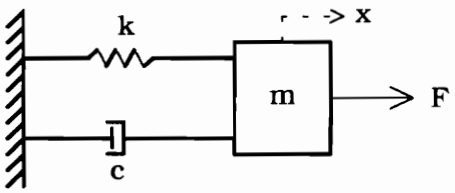

Figure A.1: Spring-Mass-Damper (SMD) Schematic

Lagrange's energy equation:

$$\frac{d}{dt}\left(\frac{\partial L}{\partial \dot{q}_i}\right)-\left(\frac{\partial L}{\partial q_i}\right)=Q_i \quad \text{where } i = 1, ..., n \text{ (n = number of generalized coordinates)}$$

generalized coordinate: $q_1 = q = x$

kinetic energy: $T = \frac{1}{2} m\dot{x}^2$, potential energy: $V = \frac{1}{2} kx^2$

Lagrangian: $L = T - V = \frac{1}{2} m\dot{x}^2 - \frac{1}{2} kx^2$

$$\frac{\partial L}{\partial x} = -kx$$

derivatives: $$\frac{\partial L}{\partial \dot{x}} = m\dot{x}$$

$$\frac{d}{dt}\left(\frac{\partial L}{\partial \dot{x}}\right) = m\ddot{x}$$

generalized force: $Q_1 = Q = F - c\dot{x}$

$\therefore$ Lagrange's equation: $m\ddot{x} + kx = F - c\dot{x}$

state-space model: $x_1 = x =$ position, $x_2 = \dot{x} =$ velocity, $\therefore$ $x_2 = \dot{x}_1$

and $m\dot{x}_2 + cx_2 + kx_1 = F$

matrix form (SSE): $$\begin{bmatrix}\dot{x}_1 \\ \dot{x}_2\end{bmatrix} = \begin{bmatrix}0 & 1 \\ -k/m & -c/m\end{bmatrix}\begin{bmatrix}x_1 \\ x_2\end{bmatrix} + \begin{bmatrix}0 \\ 1/m\end{bmatrix}F$$

Appendix B

Derivation of mode shapes for a cantilevered beam:

Euler-Bernoulli beam equation: $\frac{EI}{m}\left(\frac{\partial^4 y(x,t)}{\partial x^4}\right) = -\frac{\partial^2 y(x,t)}{\partial t^2}$

Boundary Conditions (BCs): free end: $y(0,t) = \left.\frac{\partial y}{\partial x}\right|_{x=0} = 0$

clamped end: $\left.\frac{\partial^2 y}{\partial x^2}\right|_{x=l} = \left.\frac{\partial^3 y}{\partial x^3}\right|_{x=l} = 0$

Assume: $y(x,t) = \sum_{n=1}^{\infty} r_n(t)\Psi_n(x)$ (modal analysis assumption, n=mode number)

Combining this and the beam equation yields an infinite set of differential equations:

$\beta r_n(t)\Psi_n''''(x) = -\ddot{r}_n(t)\Psi_n(x), \quad n = 1,2,\ldots,\infty, \quad \text{where } \beta = \frac{EI}{m}$

Assume a time solution of the form: $r_n(t) = e^{\alpha_n t}$

$\therefore \quad \beta\Psi_n'''' = -\alpha_n^2\Psi_n \quad \text{or} \quad \beta\Psi_n'''' = \lambda_n\Psi_n$

The solution form of this ordinary differential equation (ODE) is:

$\Psi_n(x) = C_1\sin(\mu_n x) + C_2\cos(\mu_n x) + C_3\sinh(\mu_n x) + C_4\cosh(\mu_n x)$

where $\mu_n^4 = \lambda_n / \beta$

Applying the BCs to the mode shape yields the following matrix equation:

$$\begin{bmatrix} 0 & 1 & 0 & 1 \\ 1 & 0 & 1 & 0 \\ -\sin(\mu_n l) & -\cos(\mu_n l) & \sinh(\mu_n l) & \cosh(\mu_n l) \\ -\cos(\mu_n l) & \sin(\mu_n l) & \cosh(\mu_n l) & \sinh(\mu_n l) \end{bmatrix} \begin{bmatrix} C_1 \\ C_2 \\ C_3 \\ C_4 \end{bmatrix} = \begin{bmatrix} 0 \\ 0 \\ 0 \\ 0 \end{bmatrix}$$

In order for the C constants to exist, the coefficient matrix must be singular:

$$\begin{vmatrix} 0 & 1 & 0 & 1 \\ 1 & 0 & 1 & 0 \\ -\sin(\mu_n l) & -\cos(\mu_n l) & \sinh(\mu_n l) & \cosh(\mu_n l) \\ -\cos(\mu_n l) & \sin(\mu_n l) & \cosh(\mu_n l) & \sinh(\mu_n l) \end{vmatrix} = 0 \quad \Rightarrow \quad 1 + \cos(\mu_n l)\cosh(\mu_n l) = 0$$

$\therefore \quad \mu_n l = 1.8751041,\ 4.6940911,\ 7.8547574,\ 10.995541,\ 14.137168 \quad$ for n = 1,...,5

and $\mu_n l = (2n-1)\frac{\pi}{2} \quad$ for $n < 5$

Solving for the C constants yields:

$$C_1 = \frac{\cosh(\mu_n l) + \cos(\mu_n l)}{\sinh(\mu_n l) + \sin(\mu_n l)}, \quad C_2 = -1, \quad C_3 = -C_1, \quad C_4 = -C_2$$

Therefore, the mode shapes are:

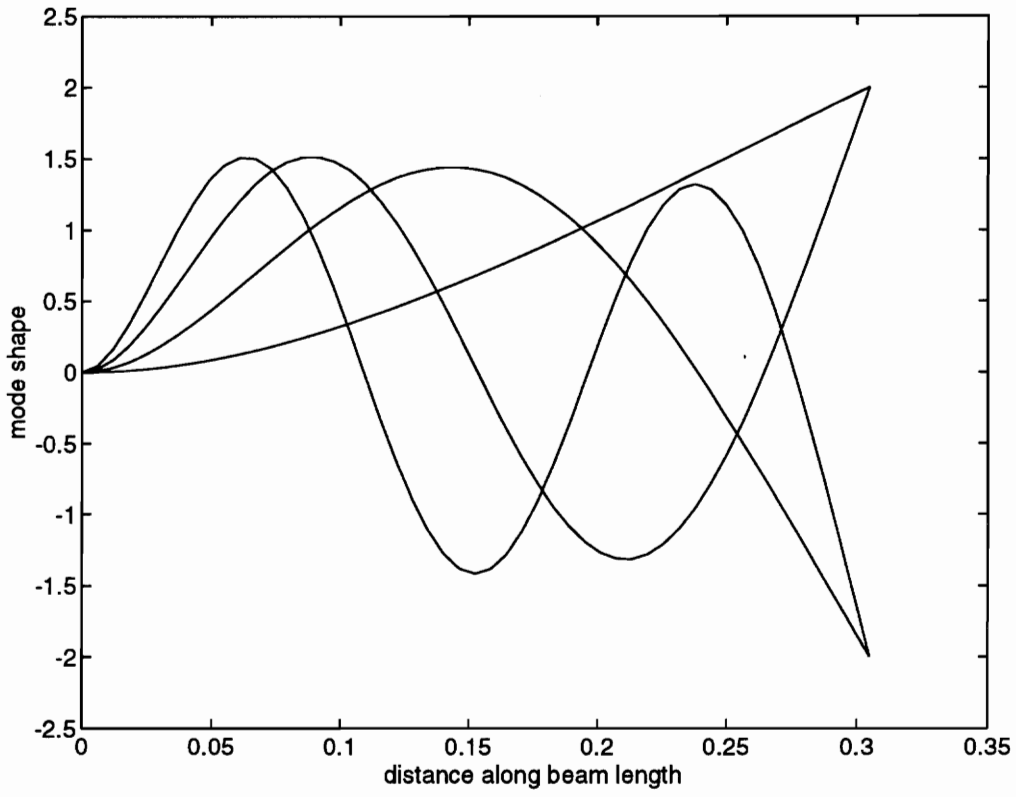

Figure B.1: First Four Mode Shapes for a Cantilevered Beam

Appendix C

ENERGY1A.M

```
%Investigation of power and energy flow in a controlled simple system:
% - This is the one mass-one damper-one spring system.
% - The states (position and velocity) are fed back to control the mass.
% - The viscous damper (f=cv) and linear spring (f=kx) act in parallel.
% - The integration scheme used here is Simpson's 1/3 Rule.
% - Where does the system's initial energy go?

clear F P U H X intp KE PE t intu
clc
help energy1a

% Set up the sampling rate
tf = input(' final time in seconds, tf =  '); % final time - sec
done='no ';
while done=='no ',
 disp(blanks(1)')
 disp([' Enter the desired number of samples between 0 and',...
 num2str(tf),' seconds.'])
 disp(' note: this must be an odd number')
 n = input(' n =  ');                    % no. of samples
 if round((n-1)/2) == (n-1)/2,           % This test is necessary
  disp(blanks(1)')                       % because of the integration
  done='yes';                            % scheme
 end
end
T=tf/(n-1);                              % sampling period - sec

% Set up the system model
m=1;                                     % mass - kg
k = input(' spring constant, k = ');     % spring constant - N/m
z = input(' damping ratio, z = ');       % damping ratio
wn = eig(inv(m)*k);                      % natural frequency - rad/sec
c = 2*z*wn*m;                            % damping coefficient - N/m/sec
A=[0 1;-k/m -c/m];
B=[0;1/m];

% Discretize the system
[phi, gamma]=c2d(A,B,T);

% Initialize the vectors (at t=0)
X(:,1) = [-1;-1/2];              % State vector
KE(1) = 1/2*m*(X(2,1))^2;        % Initial Kinetic Energy
PE(1) = 1/2*k*(X(1,1))^2;        % Initial Potential Energy
H(1) = KE(1) + PE(1);            % Total initial conservative energy
```

```
% Ask the user which pole placement method to use.
quiz = input(' DLQR or PLACE ?  ','s');
disp(blanks(1)')
if length(quiz) == 4,
 if quiz == 'dlqr' | quiz == 'DLQR',

  % Find the gain vector using Linear Quadratic Regulator Design (dlqr)
  disp(blanks(1)')
  disp('  the state weighting matrix is ')
  disp(blanks(1)')
  format compact
  Q = eye(size(phi))
  format loose
  R = input('  control weighting constant, r =  ');
  [K,S,E] = dlqr(phi,gamma,Q,R);
  clear S E

  else
  error('answer entered incorrectly')
 end
elseif length(quiz) == 5,
 if quiz == 'PLACE' | quiz == 'place',

  % Find the gain vector using linear state feedback (place)
  sroots = [-1,-2];
  zroots = exp(sroots*T);
  K = place(phi,gamma,zroots);

  else
  error('answer entered incorrectly')
 end
 else
 error('answer entered incorrectly')
end

% Simulate the controlled system response
for i=1:n,
 F(i) = -K*X(:,i);                              % N
% if F(i) > 0.5,
%  F(i) = 0.5;
% end
% if F(i) < -0.5,
%  F(i) = -0.5;
% end
 P(i) = [0 F(i)]*X(:,i);                        % power to/from source
 U(i) = c*X(2,i)^2;                             % power dissipated in damper
 if i~=n,
  X(:,i+1) = phi*X(:,i) + gamma*F(i);           % [m m/sec]
  KE(i+1) = 1/2*m*(X(2,i+1))^2;                 % Kinetic Energy
  PE(i+1) = 1/2*k*(X(1,i+1))^2;                 % Potential Energy
  H(i+1) = KE(i+1) + PE(i+1);                   % stored energy
  if H(i+1) >= 0.01*H(1),                       % 1% energy settling time
   h=i+1;
  end
 end
end
```

```
% Power integration scheme - Simpson's 1/3 rule
intp = integral(T,P);           % Energy into or out of the source
intu = integral(T,U);           % Energy transferred by damper

% Plot the results
clg
t = [0:n-1]*T;
subplot(211)
plot(t,H,'y',t,KE,'m:',t,PE,'c--',t,zeros(n,1),'w')
xlabel('time')
ylabel('Stored energy')
title('System Energy')
v=axis;
hold on
legend(.6,.9,'Total Energy','y')
legend(.6,.8,'K.E.',':m')
legend(.6,.7,'P.E.','--c')
if T*h <= tf,
 text(.45*(v(2)-v(1))+v(1),.59*(v(4)-v(3))+v(3),...
 ['energy settling time (1%) = ',num2str(T*h)])
else
 text(.6*(v(2)-v(1))+v(1),.575*(v(4)-v(3))+v(3),...
 'energy has not settled to')
 text(.6*(v(2)-v(1))+v(1),.47*(v(4)-v(3))+v(3),...
 '1% of the initial value')
end
hold off
subplot(223)
plot(t,X(1,:),'y',t,X(2,:),'m--')
title('Outputs')
xlabel('time')
ylabel('states')
legend(.4,.22,'displacement','y')
legend(.4,.12,'velocity','--m')
subplot(224)
plot(t,F,'y',t,X(2,:),'m--')
title('Input Power Variables')
xlabel('time')
ylabel('magnitude')
v=axis;
text(0.86*(v(2)-v(1))+v(1),-.27*(v(4)-v(3))+v(3),'energy1a.m')
legend(.6,.22,'force','y')
legend(.6,.12,'velocity','--m')
figure(gcf)
pause
clg
subplot(111)
axis;
plot(t,P,'m',t,U,'c-.',t(1:2:n),intp(1:2:n),'r:',t(1:2:n),...
intu(1:2:n),'g--',t,zeros(n,1),'w')
xlabel('time (seconds)')
ylabel('power/pnergy (Watts/Joules)')
title('Power/Energy IC Response')
v=axis;
hold on
```

```
%string1=['Int(P) = ',num2str(intp(n)),', IC Energy = ',num2str(H(1))...
%,', Int(U) = ',num2str(intu(n)),', n = ',num2str(n)];
%text(.05*(v(2)-v(1))+v(1),.95*(v(4)-v(3))+v(3),string1)
if k~=0,
 legend(.5,.4,'power into/out of source','m')
 legend(.5,.3,'energy into/out of source',':r')
end
if c~=0,
 legend(.5,.35,'power into/out of damper','-.c')
 legend(.5,.25,'energy into/out of damper','--g')
end
text(0.92*(v(2)-v(1))+v(1),-.1*(v(4)-v(3))+v(3),'energy1a.m')
pause
hold off
```

BEAM1.M

```
% This code finds the stiffness, mass, coupling and capacitance matrices
% from the first four mode shapes for a cantilevered beam with surface
% mounted piezoelectrics according to the theory in the Hagood, Chung
% and von Flotow paper.
%
% Simpson's 1/3 Rule integration is used in the function integral.m
% which is called by this script file.  This script file also calls the
% functions mshape.m and mshaped.m which contain the cantilevered beam
% mode shape and mode shape derivative.
%
%                                                    Darrell S. McAlister
%                                                    July 25, 1994

% Initialization
clc
help beam1
clear

% Beam (structure) properties
l = 12*0.0254;                          % length (m)
  done='no ';
  while done=='no ',
   disp(blanks(1)')
   disp('  Enter the desired number of integration steps for the beam')
   disp('  and piezoelectrics. Note: This must be an even number.')
   n = input('    n =  ');              % no. of integration steps
   if round(n/2) == n/2,                % This test is necessary
    disp(blanks(1)')                    % because of the integration
    done='yes';                         % scheme (Simpson's 1/3 rule)
   end
  end
Ts = (l-0)/n;                           % Beam integration step (m)
Es = 1.4832E9/12^2*6895;                % elastic modulus (Pa)
vs = 0.334;                             % poisson's ratio
hs = 1*0.0254;                          % height (m)
ts = (1/16)*0.0254;                     % thickness (m)
ws = (0.1*12^3)*16.02;                  % density (kg/m^3)
Is = (1/12)*hs*ts^3;                    % area moment of inertia (m^4)
Cs = Es/((1+vs)*(1-2*vs))*[1-vs vs  vs  0    0    0     % matrix of
                           vs 1-vs vs  0    0    0     % elastic
                           vs  vs 1-vs 0    0    0     % stiffness (Pa)
                           0   0   0 1/2-vs 0    0     % for isotropic
                           0   0   0   0  1/2-vs 0     % materials
                           0   0   0   0    0 1/2-vs]; % (T=Cs*S)

% Piezoelectric geometry properties
% Note that some properties are shared by both piezoelectrics
disp(blanks(1)')
np = 2;                                 % number of piezos on the beam
a(1,1) = 1.4*0.0254;                    % endpoints of piezo #1 (m)
a(1,2) = 9.4*0.0254;
a(2,1) = 0.1*0.0254;                    % endpoints of piezo #2 (m)
```

```
a(2,2) = 1.1*0.0254;
tp(1) = 0.02*0.0254;
tp(2) = 0.01*0.0254;
for i = 1:np,
 Tp(i) = (a(i,2)-a(i,1))/n;          % piezo integration step (m)
% tp(i) = 0.01*0.0254;               % thickness of piezo (m)
 hp(i) = 1*0.0254;                   % width of piezo (m)
 Ip(i) = (2/3)*hs*((ts/2+tp(i))^3-(ts/2)^3); % area moment of inertia
 Sp(i) = hs*((ts/2+tp(i))^2-(ts/2)^2);       % first area moment (m^3)
end

% Piezo -> beam coordinate transformation matrices
Rs = [1  0  0  0  0  0              % strain rotation matrix
      0  0  1  0  0  0
      0  1  0  0  0  0
      0  0  0  0  0  1
      0  0  0  0 -1  0
      0  0  0 -1  0  0];

Re = [1  0  0                       % electrical field rotation matrix
      0  0  1
      0 -1  0];

% Piezoelectric material properties
% Note that all properties are shared by both piezoelectrics
wp = 7.6E3;                         % density of piezo (kg/m^3)
vp = 0.4;                           % poisson's ratio (x-y relation)
Epx = 5.292e10;                     % elastic modulus in x & z-dir (Pa)
Epy = 4.8e10;                       % elastic modulus in y-dir (Pa)
dp = [   0       0       0    0 0 0  % strain constant matrix (m/V)
         0       0       0    0 0 0
      180e-12 180e-12 360e-12 0 0 0];
Cp = 1/(-1+vp^2)*[-Epx -vp*Epx   0       0  0  0   % matrix of elastic
                  -vp*Epx -Epx   0       0  0  0   % stiffness (Pa) for
                      0    0 (-1+vp^2)*Epy 0  0  0   % material of
                      0    0       0       0  0  0   % hexagonal symmetry
                      0    0       0       0  0  0   % T=Cp*S
                      0    0       0       0  0  0];
Dp = diag([0 0 1700*8.854e-12])-dp*Cp*dp';       % matrix of dielectric
                                                 % constants (F/m)
ep = [0 -1 0]*Re'*Dp*Re*[0 -1 0]';
ehat = [0 1 0]'*[-1 vp 0 0 0 0]*Rs'*Cp*dp'*Re*[0 -1 0]';
Cphat = [-1 vp 0 0 0 0]*Rs'*Cp*Rs*[-1 vp 0 0 0 0]';
Cshat = [-1 vs 0 0 0 0]*Cs*[-1 vs 0 0 0 0]';

% Weighted frequencies (wave numbers/l)
u(1) = 1.875104069/l;                    % 1/m
u(2) = 4.694091133/l;                    % 1/m
u(3) = 7.854757438/l;                    % 1/m
u(4) = 10.99554073/l;                    % 1/m
m=length(u);

% Calculations for piezo mass, stiffness, coupling and capacitance
% matrices (Mp, Kp, Phi and Cap).
Mp = zeros(m,m);
Kp = zeros(m,m);
```

```
Phi = zeros(m,np);
Cap = zeros(np,np);
for pindex = 1:np,
 % Mode Shape (piezo length) Function Definition for Simpson's 1/3 rule
 clear P Pdd
 for i = a(pindex,1):Tp(pindex):a(pindex,2),
  j = (i-a(pindex,1)+Tp(pindex))/Tp(pindex);
  for k=1:m,
   P(j,k) = mshape(i,k,1,u);
   Pdd(j,k) = mshaped(i,k,1,u);
  end
 end

 % Calculations for piezo mass, stiffness, coupling and capacitance
 % matrices (Mpi, Kpi, Phii and Capi).
 for i = 1:m,
  for j = 1:m,
   temp = integral(Tp(pindex),P(:,i).*P(:,j));
   eval(['Mp' num2str(pindex) '(i,j) = temp(length(temp));'])
   eval(['Kp' num2str(pindex) '(i,j) = u(i)^2*u(j)^2*Mp'...
   num2str(pindex) '(i,j);'])
  end
  temp = integral(Tp(pindex),Pdd(:,i));
  eval(['Phi' num2str(pindex) '(i,1) = temp(length(temp));'])
 end
 thick = zeros(1,np);
 thick(1,pindex) = 1/tp(pindex);
 thickt = thick';
 eval(['Phi' num2str(pindex) ' = Phi' num2str(pindex) '*thick;'])
 eval(['Cap' num2str(pindex) ' = (a(pindex,2)-a(pindex,1))...
 *thickt*thick;'])
 clear thick thickt temp

 % Summation of the piezo mass, stiffness, coupling and capacitance
 % matrices into total piezo mass, stiffness, coupling and capacitance
 % matrices.  Also, constant (along the x-dir) material properties that
 % were excluded from the integrals are multiplied here.
 eval(['Kp = Kp+Ip(pindex)*Cphat*Kp' num2str(pindex) ';'])
 eval(['Mp = Mp+wp*2*tp(pindex)*hp(pindex)*Mp' num2str(pindex) ';'])
 eval(['Phi = Phi+Sp(pindex)*ehat(2,1)*Phi' num2str(pindex) ';'])
 eval(['Cap = Cap+ep*2*tp(pindex)*hp(pindex)*Cap' num2str(pindex) ';'])
end

% Mode Shape Function Definition for Simpson's 1/3 rule - Beam
clear P temp
for i = 0:Ts:1,
 j = (i-0+Ts)/Ts;
 for k=1:m,
  P(j,k) = mshape(i,k,1,u);
 end
end

% Mode shape plots
figure
hold on
for k=1:m,
```

```
 plot([0:Ts:1],P(:,k))
end
set(gca,'box','on')
hold off
pause

% Calculation of beam mass and stiffness matrices (Ms and Ks)
for i = 1:m,
 for j = 1:m,
  temp = integral(Ts,P(:,i).*P(:,j));
  Ms(i,j) = temp(length(temp));
  Ks(i,j) = u(i)^2*u(j)^2*Ms(i,j);
 end
end
Ms = ws*hs*ts*Ms;
Ks = Is*Cshat*Ks;

% Results
M = Ms + Mp
K = Ks + Kp

% Damping Matrix
wn=sort(sqrt(eig(inv(M)*K)));  % natural freqs sorted in acsending order
z=0.01;                        % modal damping ratio
Damp=M*diag(2*z*wn)            % damping matrix

Phi
Cap
```

BEAM2.M

```
% This code finds the beam-piezoelectrics-electronics (BPE) system
% closed loop state representations.  dX/dt = A*X + B*U and Y = C*X
% is the result for the open loop system and dX/dt = Aclosed*X is the
% results for the closed loop system.  X is the state vector.
%
% The open loop system is simulated, using lsim, with zero external
% inputs and the initial conditions specified below.
% The solution to the closed loop matrix equation is X(t)=exp(At)*X(0).
%
%                                                    Darrell S. McAlister
%                                                    December 22, 1994
%
%

% Information required (from beam1.m):
%    M    -  beam and piezo mass matrix
%    Damp -  beam and piezo damping matrix
%    K    -  beam and piezo stiffness matrix
%    Phi  -  piezoelectric electromechanical coupling matrix
%    Cap  -  piezoelectric capacitance matrix
%    Ts   -  beam intgration step
%    l    -  beam length, n=l/Ts
%    P    -  matrix of beam mode shapes

% Initialization
clc
clear T F G H J X Xo A Ar1 Ar2 Av11 Av12 Av21 Av22 denom1 denom2 vd ip
root v
help beam2
disp('  Input the simulation time interval (in seconds):')
t1 = input('    initial time = ');
t2 = input('    final time = ');
n = input([' Input the number of time steps between ',num2str(t1),...
     ' and ',num2str(t2),' seconds for simulation = ']);
T = (t2-t1)/n;              % time step
m = length(M);              % no. of modes used
X(:,1) = [0.025;0;0;0;      % initial conditions; state vector at time t1
          0;0;0;0;0;0];


% Plot the response due to initial conditions given above
% of the open loop piezostructure described by A,B,C,D above
figure
time = [t1:T:t2];
Xo(:,1) = [0.025;0;0;0;    % initial conditions; state vector at time t1
          0;0;0;0];
Ao = [zeros(m,m) eye(m,m);-M\K -M\Damp];      % actuator equation
Bo = [zeros(m,2); M\Phi];                     % inputs = piezo voltages
Co = [-inv(Cap(2,2))*Phi(:,2)' zeros(1,m)];   % sensor equation
Do = [0 0];                                   % output=pair #2 voltage de
[Yo,Xo]=lsim(Ao,Bo,Co,Do,[zeros(n+1,2)],time,Xo(:,1));
```

```
Xo=Xo';
Yo=Yo';
for i=1:n,
 if Xo(1,i+1) >= 0.05*Xo(1,1),                % 5% displacement settling
time
  h=i+1;
 end
end
figure(gcf)
plot(time,Xo(1,:),'c',time,Xo(2,:),'r',time,Xo(3,:),'g',time,Xo(4,:),'b'
v=axis;
if time(h) < t2-T,
 string=['5% settling time = ',num2str(time(h)),' seconds']
else
 string=['5% settling time > ',num2str(time(h)),' seconds']
end
text(.6*(v(2)-v(1))+v(1),.2*(v(4)-v(3))+v(3),string)
axis([t1 t2 -Xo(1,1) Xo(1,1)])
title('Open-Loop Response to IC''s')
xlabel('time (seconds)')
ylabel('modal displacement (meters)')
legend(.65,.9,'1st mode','c')
legend(.65,.85,'2nd mode','r')
legend(.65,.8,'3rd mode','g')
legend(.65,.75,'4th mode','b')
% Electronics properties
Cf = 1e-6;                  % feedback capacitance (farad, F)
Rf = 100000;                % feedback resistance (ohm)
N = -5;                     % transformer turns ratio
k = 200000;                 % op-amp open loop voltage gain
Ri = 2000000;               % op-amp input resistance (ohm)
Ro = 75;                    % op-amp output resistance (ohm)
% See Franco, 1988 for the 741 op-amp resistances and gain

% Sub-Calculations
T1 = Phi(:,1);
T2 = Phi(:,2);
Cp1 = Cap(1,1);
Cp2 = Cap(2,2);

% Root locus from piezo #1 voltage (V1) to op-amp
% output voltage (V).  States are modal displacements,
% modal velocities, V and piezo #2 voltage (V2).
figure
temp=N;
N1 = 1;
NT = -1;
N2 = -250;
B = [zeros(m,1);inv(M)*T1;0;0];
for N = N1:NT:N2,
 d = Cf-(Cf+Cp2)/Cf*(N^2*Cp1+Cf);
 Ar1 = (T2'+N*T1'*(Cf+Cp2)/Cf)/d;
 Ar2 = (N*T1'+(Cf+N^2*Cp1)/Cf*T2')/d;
 Av1 = (-1/Rf+(Cf+Cp2)/Cf*(1/Rf+1/Ro))/d;
 Av2 = (1/Rf+1/Ro-(Cf+N^2*Cp1)/Cf/Rf)/d;
 Av21 = (1/Rf+1/Ri-(Cf+Cp2)/Cf*(1/Rf-k/Ro))/d;
```

```
 Av22 = (-1/Rf+k/Ro+(N^2*Cp1+Cf)/Cf*(1/Rf+1/Ri))/d;
 A = [zeros(m,m)    eye(m)     zeros(m,1)  zeros(m,1);
      -inv(M)*K  -inv(M)*Damp  zeros(m,1)  inv(M)*T2 ;
      zeros(1,m)     Ar1          Av1         Av21   ;
      zeros(1,m)     Ar2          Av2         Av22  ];
 G = [zeros(1,2*m) N 0];
 root((N-N1+NT)/NT,:) = sort(eig(A+B*G))';
end
hold on
v=[-50 10 -5000 5000];
axis(v)
set(gca,'box','on')
plot([v(1) v(2)],[0 0],':w',[0 0],[v(3) v(4)],':w')
plot(real(root(:,1)),imag(root(:,1)),'y.')
plot(real(root(:,2)),imag(root(:,2)),'m.')
plot(real(root(:,3)),imag(root(:,3)),'m.')
plot(real(root(:,4)),imag(root(:,4)),'r.')
plot(real(root(:,5)),imag(root(:,5)),'r.')
plot(real(root(:,6)),imag(root(:,6)),'b.')
plot(real(root(:,7)),imag(root(:,7)),'b.')
plot(real(root(:,8)),imag(root(:,8)),'c.')
plot(real(root(:,9)),imag(root(:,9)),'c.')
plot(real(root(:,10)),imag(root(:,10)),'y.')
plot(real(root(1,:)),imag(root(1,:)),'xg')
title('Root Locus for V/V1')
xlabel('Real Axis')
ylabel('Imaginary Axis')
hold off
figure(gcf)
pause
N=temp;

% Controlled (closed loop) state matrix (10 by 10)
d1 = (N*Cp1+Cf/N-Cf^2/(Cf+Cp2)/N);
d2 = (Cf+Cp2-Cf^2/(Cf+N^2*Cp1));
Ar1 = (-N*T1'-Cf*T2'/(Cf+Cp2))/d1;
Ar2 = (-T2'-Cf*N*T1'/(Cf+N^2*Cp1))/d2;
Av22 = -(1/Ri+1/Rf+(Cf*k/Ro-Cf/Rf)/(Cf+N^2*Cp1))/d2;
Av21 = -(k/Ro-1/Rf+(Cf/Ri+Cf/Rf)/(Cf+Cp2))/d1;
Av12 = (1/N/Rf-(Cf/N/Rf+Cf/N/Ro)/(Cf+N^2*Cp1))/d2;
Av11 = (-1/N/Rf-1/N/Ro+Cf/(Cf+Cp2)/N/Rf)/d1;
Aclosed = [zeros(m,m)   eye(m)        zeros(m,2)     ;
           -inv(M)*K -inv(M)*Damp inv(M)*T1 inv(M)*T2;
           zeros(1,m)    Ar1        Av11      Av21   ;
           zeros(1,m)    Ar2        Av12      Av22  ];

% Solve the BPE system subject to the given I.C.'s

% Solve the SSE
for t=t1+T:T:t2,
 X(:,(t-t1+T)/T) = expm(Aclosed*(t-t1))*X(:,1);
end
```

```
for i=1:n,
 if X(1,i+1) >= 0.05*X(1,1),                % 5% displacement settling
time
  h=i+1;
 end
end

% Solve for charges and currents
vd = Aclosed(9:10,1:10)*X;                  % patch voltage derivatives
for t=t1:T:t2,
 ip(1,(t-t1+T)/T) = T1'*X(5:8,(t-t1+T)/T)+Cp1*vd(1,(t-t1+T)/T);
 ip(2,(t-t1+T)/T) = T2'*X(5:8,(t-t1+T)/T)+Cp2*vd(2,(t-t1+T)/T);
 q(1,(t-t1+T)/T) = T1'*X(1:4,(t-t1+T)/T)+Cp1*X(9,(t-t1+T)/T);
 q(2,(t-t1+T)/T) = T2'*X(1:4,(t-t1+T)/T)+Cp2*X(10,(t-t1+T)/T);
end

figure
hold off
plot(time,X(1,:),'c',time,X(2,:),'r',time,X(3,:),'g',time,X(4,:),'b')
title('Closed-Loop Response to IC''s')
xlabel('time (seconds)')
ylabel('modal displacement (meters)')
v=axis;
if time(h) < t2-T,
 string=['5% settling time = ',num2str(time(h)),' seconds']
else
 string=['5% settling time > ',num2str(time(h)),' seconds']
end
text(.6*(v(2)-v(1))+v(1),.2*(v(4)-v(3))+v(3),string)
legend(.65,.9,'1st mode','c')
legend(.65,.85,'2nd mode','r')
legend(.65,.8,'3rd mode','g')
legend(.65,.75,'4th mode','b')
axis([t1 t2 -X(1,1) X(1,1)])
figure(gcf)
pause
plot(time,X(5,:),'c',time,X(6,:),'r',time,X(7,:),'g',time,X(8,:),'b')
title('Closed-Loop Response to IC''s')
xlabel('time (seconds)')
ylabel('modal velocity (m/s)')
pause
plot(time,X(9,:),'c',time,X(10,:),'--b')
title('Closed-Loop Response to IC''s')
xlabel('time (seconds)')
ylabel('patch voltage (Volts)')
legend(0.7,0.3,'pair #1','c')
legend(0.7,0.25,'pair #2','--b')
pause
plot(time,ip(1,:),'c',time,ip(2,:),'--b')
title('Closed-Loop Response to IC''s')
xlabel('time (seconds)')
ylabel('patch current (Amps)')
legend(0.7,0.3,'pair #1','c')
legend(0.7,0.25,'pair #2','--b')
pause
```

BEAM2O.M

```
% Given the beam-piezoelectrics-electronics (BPE) system open-loop
% state representation, this code solves for the response to initial
% conditions. X is the vector of modal displacements and velocities.
% The response is found using lsim with zero inputs and the prescribed
% initial conditions. This code also finds the open-loop power flow and
% energy transfer.
%
%                                                    Darrell S. McAlister
%                                                    October 31, 1994
%
%
%
% Power sign convention:
%      Resistive, Capacitive or Inertial primitives
%           + energy into the primitive
%           - energy out of the primitive
%      Sources
%           + energy out of the primitive
%
%

% Information required (from beam1.m):
%    M    -  beam and piezo mass matrix
%    Damp -  beam and piezo damping matrix
%    K    -  beam and piezo stiffness matrix
%    Phi  -  piezoelectric electromechanical coupling matrix
%    Cap  -  piezoelectric capacitance matrix
%    Ts   -  beam intgration step
%    l    -  beam length, n=l/Ts

% Initialization
clc
clear Tr T Tv Xo Yo X0 KE PE Pd Ed
help beam2o
disp('  Input the simulation time interval (in seconds):')
t1 = input('    initial time = ');
t2 = input('    final time = ');
n = input([' Input the number of time steps between ',num2str(t1),...
     ' and ',num2str(t2),' seconds for simulation = ']);
m = length(M);
Tv = linspace(t1,t2,n+1);   % time vector
T = (t2-t1)/n;              % time step
X0 = [0.025 0 0 0 0 0 0 0]; % initial conditions; state vector at time
t1

% Open-loop piezostructure state representation
% The states are the coupled modal displacements and velocities
Ao = [zeros(m,m) eye(m,m);-M\K -M\Damp];     % actuator equation
Bo = [zeros(m,2); M\Phi];                    % inputs = piezo voltages
Co = [-inv(Cap(2,2))*Phi(:,2)' zeros(1,m)];  % sensor equation
Do = [0 0];
```

```
% Plot the magnitude of the open loop piezostructure
% The states are the modal displacements and velocities
w = linspace(10*2*pi,1000*2*pi,700);
[mag,phase] = bode(Ao,Bo,Co,Do,1,w);
semilogx(w/(2*pi),mag(:,1))
title('Piezostructure Bode Plot')
xlabel('frequency, Hz.')
ylabel('magnitude of v1')

% Transform coupled system matrices to uncoupled system matrices
% The states are the uncoupled modal displacements and velocities
Tr=basis(Ao);
Aou=mxfilter(inv(Tr'*Tr)*Tr'*Ao*Tr,1e-4);
Bou=mxfilter(inv(Tr'*Tr)*Tr'*Bo,1e-12);
Cou=mxfilter(Co*Tr,1e-12);
Dou=Do;

% Open-Loop Time Simulation of uncopuled system
[Yo,Xo]=lsim(Aou,Bou,Cou,Dou,zeros(n+1,2),Tv,X0);
Xo=Xo';
Yo=Yo';
hold off
time = [t1:T:t2];
plot(time,Xo(1,:),'c',time,Xo(3,:),'r',time,Xo(5,:),'g',time,Xo(7,:),'b'
title('Open-Loop Response to IC''s')
xlabel('time (seconds)')
ylabel('modal displacement (m)')
axis([t1 t2 -Xo(1,1) Xo(1,1)])
figure(gcf)
pause
plot(time,Xo(2,:),'c',time,Xo(4,:),'r',time,Xo(6,:),'g',time,Xo(8,:),'b'
title('Open-Loop Response to IC''s')
xlabel('time (seconds)')
ylabel('modal velocity (m/s)')
figure(gcf)
pause

% Open-Loop Time Simulation of copuled system
[Yo,Xo]=lsim(Ao,Bo,Co,Do,zeros(n+1,2),Tv,X0);
Xo=Xo';
Yo=Yo';

% Mechanical Energy (beam) (Joules)
for i=1:n+1,
 KE(i) = 1/2*Xo(5:8,i)'*M*Xo(5:8,i);        % kinetic energy
 PE(i) = 1/2*Xo(1:4,i)'*K*Xo(1:4,i);        % potential energy
end
H = KE + PE;                                % total mechanical energy

% Power out of beam due to damping in all modes
for i=1:n+1,
 Pd(i) = Xo(5:8,i)'*Damp*Xo(5:8,i);
end

% Energy out of beam due to modal damping
Ed = integral(T,Pd);
```

```
% Plots
time = [t1:T:t2];
figure
hold off
plot(time,Xo(1,:),'c',time,Xo(2,:),'r',time,Xo(3,:),'g',time,Xo(4,:),'b'
title('Open-Loop Response to IC''s')
xlabel('time (seconds)')
ylabel('modal displacement (m)')
axis([t1 t2 -Xo(1,1) Xo(1,1)])
figure(gcf)
pause
plot(time,Xo(5,:),'c',time,Xo(6,:),'r',time,Xo(7,:),'g',time,Xo(8,:),'b'
title('Open-Loop Response to IC''s')
xlabel('time (seconds)')
ylabel('modal velocity (m/s)')
pause
time=[t1:2*T:t2];
v2=integral(T,Yo);
plot(time,v2(1:2:length(v2)))
title('Open-Loop Response to IC''s')
xlabel('time (seconds)')
ylabel('piezo #2 voltage (Volts)')
pause
plot([t1:T:t2],Pd)
title('Damping Power Dissipation')
xlabel('time (seconds)')
ylabel('power (Watts)')
pause
plot(time,Ed(1:2:n+1),'y',[t1:T:t2],H,'--m')
title('Damper Energy Dissipation')
xlabel('time (seconds)')
ylabel('energy (Joules)')
legend(.4,.25,'system energy (T+V)','--m')
legend(.4,.15,'damping energy','y')
v=axis;
string1=['Total Energy Out = ',num2str(Ed(n+1)),...
',  IC Energy = ',num2str(H(1)),',  Np = ',num2str(n)];
text(.2*(v(2)-v(1))+v(1),.35*(v(4)-v(3))+v(3),string1)
```

BEAM3.M

```
% This code finds the power flow and energy transfer in the beam, piezo
% and electronics system from the information found in beam1.m
% (M,C,K,Phi and Cap matrices) and beam2.m (piezo electrode voltage time
% histories as a result of I.C.'s).
%
% This script file calls the function integral.m to integrate the power
% curves.
%
% Power sign convention:
%      Resistive, Capacitive or Inertial primitives
%           + energy into the primitive
%           - energy out of the primitive
%      Sources
%           + energy out of the primitive
%

% Information required (from beam2.m):
%  X  - vector of modal displacements, velocities and piezo voltages
%  M,Damp,K - BPE system mass, damping and stiffness matrices
%  Ri - op-amp input resistance
%  Ro - op-amp output resistance
%  k  - op-amp open loop gain
%  N  - transformer turns ratio
%  Rf - feedback resistance
%  Cf - feedback capacitance
%  Aclosed - closed loop state matrix (10x10) used
%            to calculate dv/dt and d/dt(dx/dt)
%  t1,t2,T - initial time, final time, time step (between samples in X)
%  n - number of time steps between t1 and t2

% Initialization
clc
clear i Pi Ei Po Eo Pr Er Pd Ed Pc Ec Pv Ev KP PP KE PE PT E PH H Ediff
Pdiff
help beam3

% patch voltage derivatives
vd = Aclosed(9:10,1:10)*X;

% Power calculations (Watts - Joules/s)
Pi = X(10,:).^2/Ri;                          % power lost in Ri
Po = (-k*X(10,:)-X(9,:)/N).^2/Ro;            % power lost in Ro
Pr = (X(10,:)-X(9,:)/N).^2/Rf;               % power lost in Rf
Pc = Cf*([-1/N 1]*X(9:10,:)).*([1 -1/N]*vd);  % power into/out of Cf
Pv = -k*X(10,:).*(-k*X(10,:)-X(9,:)/N)/Ro;    % power into/out of Vo
for i=1:n+1,
 Pd(i) = X(5:8,i)'*Damp*X(5:8,i);     % power out of beam due to damping
end

% Beam Mechanical Energy (Joules) and Power (Watts) (reactive)
for i=1:n+1,
 KE(i) = 1/2*X(5:8,i)'*M*X(5:8,i);  % kinetic energy
 PE(i) = 1/2*X(1:4,i)'*K*X(1:4,i);  % potential energy
```

```
 KP(i) = (X(5:8,i))'*M*(Aclosed(5:8,1:10)*X(:,i)); % kinetic power
 PP(i) = (X(5:8,i))'*K*X(1:4,i);    % potential power
end
H = KE + PE;                        % total mechanical energy
PH = KP +PP;                        % total mechanical power

% Energy calculations (integral of power) (Joules)
Ei = integral(T,Pi);                % energy lost in Ri
Eo = integral(T,Po);                % energy lost in Ro
Er = integral(T,Pr);                % energy lost in Rf
Ed = integral(T,Pd);                % energy lost due to beam damping
Ec = integral(T,Pc);                % energy stored in/withdrawn from Cf
Ev = integral(T,Pv);                % energy stored in/withdrawn from Vo

E = Ei+Eo+Er+Ed+Ec-Ev;    % Total dissipated, stored and supplied energy
Ediff = H(1)-(H+E);       % Energy difference (ignore every other point
                          % starting with the second one)

PT = Pi+Po+Pr+Pd+Pc-Pv;   % Total dissipated, stored and supplied power
Pdiff = PH(1)-(PH+PT);    % Power difference

% Results
time=[t1:T:t2];
figure
plot([t1:2*T:t2],E(1:2:n+1)','r',time,H,':m')
title('total energy flow')
xlabel('time (seconds)')
ylabel('energy (Joules)')
legend(0.4,0.6,'total energy','r')
legend(0.4,0.55,'K.E. + P.E. (beam - reactive energy)',':m')
v=axis;
string=['Diss. Energy = ',num2str(E(n+1)),...
' J, IC Energy = ',num2str(H(1)),' J, n = ',num2str(n+1)];
text(.2*(v(2)-v(1))+v(1),.7*(v(4)-v(3))+v(3),string)
pause
plot([t1:2*T:t2],Ediff(1:2:n+1),':c')
title('energy difference between reactive and dissipated')
xlabel('time (seconds)')
ylabel('energy (Joules, N-m)')
pause
plot(time,Pi,'c',[t1:2*T:t2],Ei(1:2:n+1)','--b')
title('energy flowing into Ri')
xlabel('time (seconds)')
ylabel('power/energy (Watts/Joules)')
legend(0.6,0.7,'power','c')
legend(0.6,0.65,'energy','--b')
v=axis;
string=['Final Energy = ',num2str(Ei(length(Ei)))];
text(.6*(v(2)-v(1))+v(1),.58*(v(4)-v(3))+v(3),string)
pause
plot(time,Po,'-c',[t1:2*T:t2],Eo(1:2:n+1)','--b')
title('energy flowing into Ro')
xlabel('time (seconds)')
ylabel('power/energy (Watts/Joules)')
legend(0.6,0.7,'power','c')
legend(0.6,0.65,'energy','--b')
```

```
v=axis;
string=['Final Energy = ',num2str(Eo(length(Eo)))];
text(.6*(v(2)-v(1))+v(1),.58*(v(4)-v(3))+v(3),string)
pause
plot(time,Pr,'c',[t1:2*T:t2],Er(1:2:n+1)','--b')
title('energy flowing into Rf')
xlabel('time (seconds)')
ylabel('power/energy (Watts/Joules)')
legend(0.6,0.7,'power','c')
legend(0.6,0.65,'energy','--b')
v=axis;
string=['Final Energy = ',num2str(Er(length(Er)))];
text(.6*(v(2)-v(1))+v(1),.58*(v(4)-v(3))+v(3),string)
pause
plot(time,Pd,'c',[t1:2*T:t2],Ed(1:2:n+1)','--b')
title('energy flowing out of the beam due to damping')
xlabel('time (seconds)')
ylabel('power/energy (Watts/Joules)')
legend(0.6,0.7,'power','c')
legend(0.6,0.65,'energy','--b')
v=axis;
string=['Final Energy = ',num2str(Ed(length(Ed)))];
text(.6*(v(2)-v(1))+v(1),.58*(v(4)-v(3))+v(3),string)
pause
plot(time,Pc,'c',[t1:2*T:t2],Ec(1:2:n+1)','--b')
title('energy stored in/withdrawn from Cf')
xlabel('time (seconds)')
ylabel('power/energy (Watts/Joules)')
legend(0.6,0.7,'power','c')
legend(0.6,0.65,'energy','--b')
v=axis;
string=['Final Energy = ',num2str(Ec(length(Ec)))];
text(.6*(v(2)-v(1))+v(1),.58*(v(4)-v(3))+v(3),string)
pause
plot(time,Pv,'c',[t1:2*T:t2],Ev(1:2:n+1),'--b')
title('energy into/out of Vo')
xlabel('time (seconds)')
ylabel('power/energy (Watts/Joules)')
legend(0.6,0.7,'power','c')
legend(0.6,0.65,'energy','--b')
v=axis;
string=['Final Energy = ',num2str(Ev(length(Ev)))];
text(.6*(v(2)-v(1))+v(1),.58*(v(4)-v(3))+v(3),string)
pause
plot(time,Po+Pi-Pv,'c')
title('total op-amp power consumption')
xlabel('time (seconds)')
ylabel('power (Watts)')
```

BEAM4.M

```
% This code finds the power flow and energy transfer in the beam, piezo
% and electronics system from the information found in beam1.m
% (M,C,K,Phi and Cap matrices) and beam2.m (piezo electrode voltage time
% histories as a result of I.C.'s).  The calculations here are based on
% the "black-box" model.  This script file calls the function integral.m
% to integrate the power curves.
%
% Power sign convention:
%      Resistive, Capacitive or Inertial primitives
%           + energy into the primitive
%           - energy out of the primitive
%      Sources
%           + energy out of the primitive
%

% Information required (from beam2.m):
%  X  - vector of modal displacements, velocities and piezo voltages
%  M,C,K - BPE system mass, damping and stiffness matrices
%  Ri - op-amp input resistance
%  Ro - op-amp output resistance
%  k  - op-amp open loop gain
%  N  - transformer turns ratio
%  Rf - feedback resistance
%  Cf - feedback capacitance
%  Damp - beam/piezo viscous damping matrix
%  ip - piezoelectric electrode current vector
%  Aclosed - closed loop state matrix (10x10) used
%            to calculate dv/dt and d/dt(dx/dt)
%  t1,t2,T - initial time, final time, time step (between samples in X)
%  n - number of time steps between t1 and t2

% Initialization
clc
clear i Pi Ei Po Eo Pr Er Pd Ed Pc Ec Pv Ev PP PE KP KE PH H PT E Pdiff
help beam4
Vcc = max(max(abs(X(9,:)/N)));   % op-amp rail or supply voltage (Volts)
Iq = 1e-6;                       % quiescent supply current (Amps)

% patch voltage derivatives
vd = Aclosed(9:10,1:10)*X;

% op-amp output current
io = (X(9,:)/N+k*X(10,:))/Ro;

% Power calculations (Watts - Joules/s - N*m/s)
for i = 1:n+1,
 if io(i) < 0
  Pout = Vcc.*io-X(9,:)/N.*io;          % power out of op-amp output
 else
  Pin = X(9,:)/N.*io+Vcc.*io;           % power into of op-amp output
 end
end
```

```
Po = Pin-Pout;                              % total op-amp power
Pb = ones(1,n+1)*(Vcc-(-Vcc))*Iq;           % power needed to bias op-amp
Pamp = Pb+Po;                               % total power into/out of op-amp
                                            % positive=power into amp (sink)
Pr = (X(10,:)-X(9,:)/N).^2/Rf;              % power lost in Rf
Pc = Cf*([-1/N 1]*X(9:10,:)).*([1 -1/N]*vd); % power into/out of Cf
for i=1:n+1,
 Pd(i) = X(5:8,i)'*Damp*X(5:8,i);           % Power out due to beam damping
end

% Beam Mechanical Energy (Joules) and Power (Watts) (reactive)
for i=1:n+1,
 KE(i) = 1/2*X(5:8,i)'*M*X(5:8,i);      % kinetic energy
 PE(i) = 1/2*X(1:4,i)'*K*X(1:4,i);      % potential energy
 KP(i) = (X(5:8,i))'*M*(Aclosed(5:8,1:10)*X(:,i)); % kinetic power
 PP(i) = (X(5:8,i))'*K*X(1:4,i);        % potential power
end
H = KE + PE;                                % total mechanical,reactive energy
PH = KP + PP;                               % total mechanical,reactive power

% Energy calculations (integral of power) (Joules)
Eamp = integral(T,Pamp);        % energy into/out of op-amp
Er = integral(T,Pr);            % energy lost in Rf
Ed = integral(T,Pd);            % energy lost due to beam damping
Ec = integral(T,Pc);            % energy stored in/withdrawn from Cf

E = Eamp+Er+Ed+Ec;              % Total energy
Ediff = (H-E);                  % Energy difference (ignore every other
                                % point starting with the second one)

PT = Pamp+Pr+Pd+Pc;             % Total power
Pdiff = (PH-PT);                % Power difference

% Results
time=[t1:T:t2];
figure
plot([t1:2*T:t2],E(1:2:n+1)','y',time,H,'--m')
title('total energy flow')
xlabel('time (seconds)')
ylabel('energy (Joules, N-m)')
legend(0.4,0.6,'total energy','y')
legend(0.4,0.55,'K.E. + P.E. (beam - reactive energy)','--m')
v=axis;
string1=['Diss. Energy = ',num2str(E(n+1)),...
' J, IC Energy = ',num2str(H(1)),' J, n = ',num2str(n+1)];
text(.05*(v(2)-v(1))+v(1),.95*(v(4)-v(3))+v(3),string1)
pause
plot([t1:2*T:t2],Ediff(1:2:n+1),'c')
title('energy difference between reactive and dissipated')
xlabel('time (seconds)')
ylabel('energy (Joules, N-m)')
pause
plot(time,Pr,'c',[t1:2*T:t2],Er(1:2:n+1)','--b')
title('energy flowing into Rf')
xlabel('time (seconds)')
ylabel('power/energy (Watts/Joules)')
```

```
legend(0.6,0.7,'power','c')
legend(0.6,0.65,'energy','--b')
v=axis;
string=['Final Energy = ',num2str(Er(length(Er)))];
text(.6*(v(2)-v(1))+v(1),.58*(v(4)-v(3))+v(3),string)
pause
plot(time,Pd,'c',[t1:2*T:t2],Ed(1:2:n+1)','--b')
title('energy flowing out of the beam due to damping')
xlabel('time (seconds)')
ylabel('power/energy (Watts/Joules)')
legend(0.6,0.7,'power','c')
legend(0.6,0.65,'energy','--b')
v=axis;
string=['Final Energy = ',num2str(Ed(length(Ed)))];
text(.6*(v(2)-v(1))+v(1),.58*(v(4)-v(3))+v(3),string)
pause
plot(time,Pc,'c',[t1:2*T:t2],Ec(1:2:n+1)','--b')
title('energy stored in/withdrawn from Cf')
xlabel('time (seconds)')
ylabel('power/energy (Watts/Joules)')
legend(0.6,0.7,'power','c')
legend(0.6,0.65,'energy','--b')
v=axis;
string=['Final Energy = ',num2str(Ec(length(Ec)))];
text(.6*(v(2)-v(1))+v(1),.58*(v(4)-v(3))+v(3),string)
pause
plot(time,Pamp,'c',[t1:2*T:t2],Eamp(1:2:n+1)','--b')
title('total energy into/out of op-amp')
xlabel('time (seconds)')
ylabel('energy (Joules, N-m)')
legend(0.6,0.7,'power','c')
legend(0.6,0.65,'energy','--b')
v=axis;
string=['Final Energy = ',num2str(Eamp(length(Eamp)))];
text(.6*(v(2)-v(1))+v(1),.58*(v(4)-v(3))+v(3),string)
```

Vita

Darrell McAlister was born on March 14, 1969 in Waynesboro, Va. After high school, he attended Old Dominion University in Norfolk, Va. where, in May of 1992, he received a Bachelor of Science Cum Laude in Mechanical Engineering. Upon entering the master's program at Va. Tech, Darrell received a departmental assistantship in the CAD/CAM lab as well as pursuing research in the controls field. After two and a half agonizing years he received his Master of Science in Mechanical Engineering. Next, he plans to pursue a career as a design engineer or win the lottery and live a life of luxury with no worries.